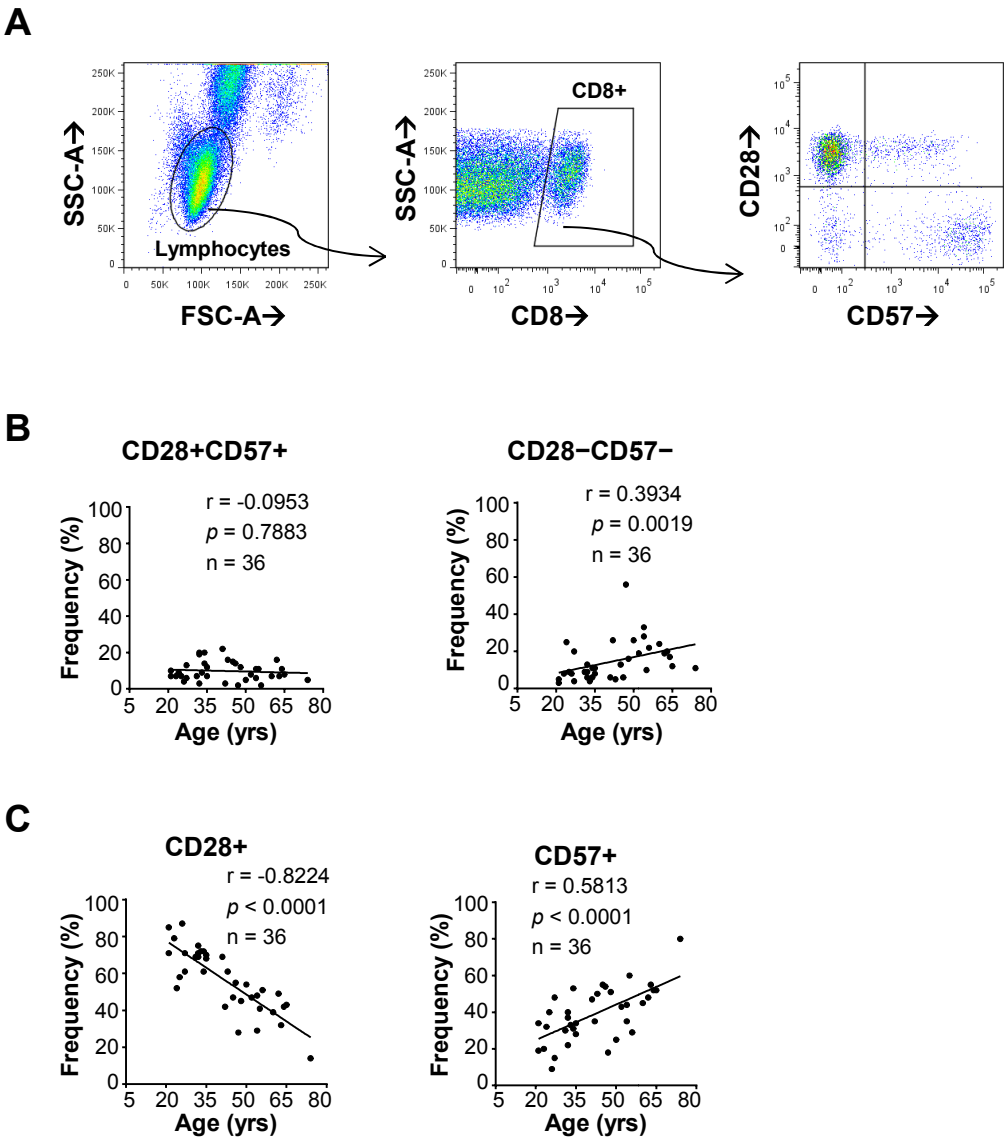

Supplemental Figure 1

Association of CD28 and CD57 expression with age. (**A**) Representative dot plots of flow cytometric analysis (Donor-27). Freshly isolated lymphocytes from the peripheral blood from healthy donors were stained with anti-CD8-FITC, anti-CD28-APC, anti-CD57-PE and 7-AAD (for viability), and analyzed by flow cytometry. (Left) The gate indicates viable lymphocytes. (Middle) $CD8^+$ lymphocytes were gated from the total lymphocytes. (Right) CD28/CD57 quadrants were gated from $CD8^+$ lymphocytes, based on fluorescence-minus-one stained controls. (**B**) Frequency of the $CD28^+CD57^+$ (Left) and $CD28^-CD57^-$ (Right) subsets of $CD8^+$ T lymphocytes with donor age (n = 31). (**C**) Frequency of the $CD28^+$ (Left) and $CD57^+$ (Right) subsets of $CD8^+$ T lymphocytes with donor age (n = 31).

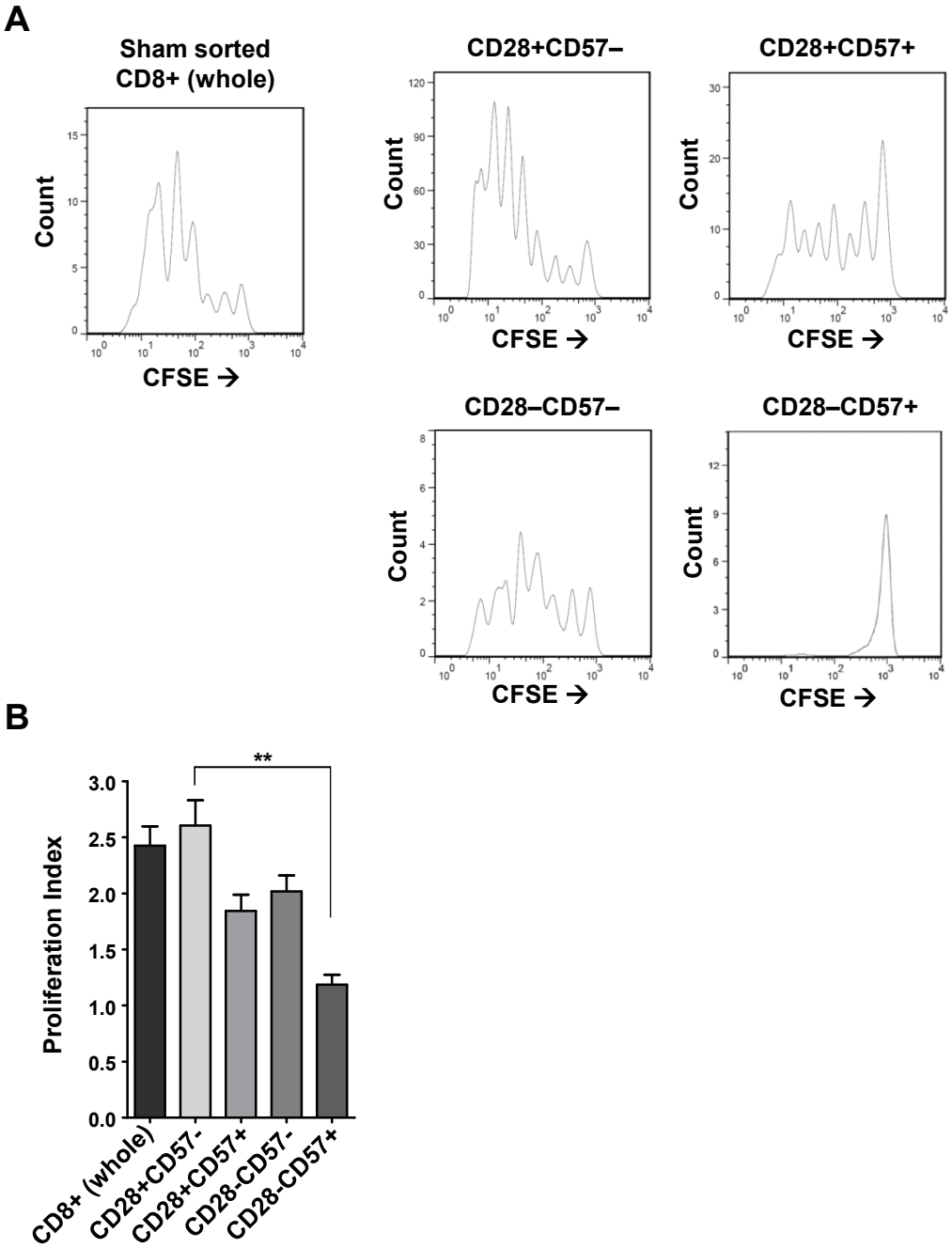

Supplemental Figure 2

Proliferative potential of the FACS-sorted populations. Blood $CD8^+$ T lymphocytes were sorted into four populations based on their CD28 and CD57 expression. The sorted cells were stained with CFSE, followed by stimulation with PHA and rIL2. After 5 days in culture the cells were stained with anti-CD8-APC-Cy7, anti-CD28-APC, anti-CD57-PE and 7-AAD, and analyzed by flow cytometry. (**A**) Representative proliferation histograms of the sham-sorted whole $CD8^+$ T lymphocytes and their four subsets. The rightmost peak corresponds to undivided cells. The leftward shift of peaks represents number of cell divisions. Most of the $CD28^+CD57^-$ cells underwent more than 4 cell divisions (Upper, Middle), whereas the majority of $CD28^-CD57^+$ cells did not undergo any cell divisions (Lower, Right). (**B**) Quantitative data summary of the proliferative indexes in the sham-sorted whole $CD8^+$ T lymphocytes and their CD28/CD57 quadrants. The proliferative indexes were determined as described in Methods section. Data are mean ± SD from three donors (Donors 16-18). $^{**}P < 0.01$.

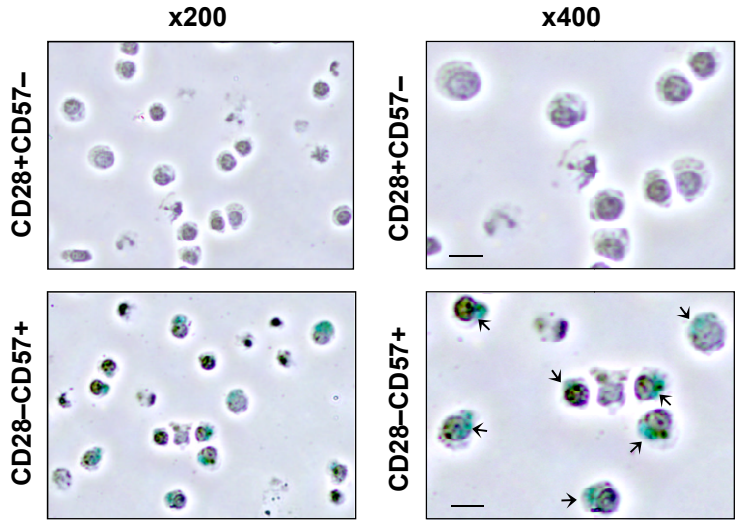

Supplemental Figure 3

CD28^{-}CD57^{+} subsets show increased SA-β-gal activity. Representative SA-β-gal staining in the FACS-sorted CD28^{+}CD57^{-} and CD28^{-}CD57^{+} subsets of CD8^{+} T lymphocytes at 200 times and 400 times of magnification (Donor-4). Cytoplasmic staining for SA-β-gal activity in the CD28^{-}CD57^{+} subset was marked using arrows in the right panel. Scale bars: 10 μm.

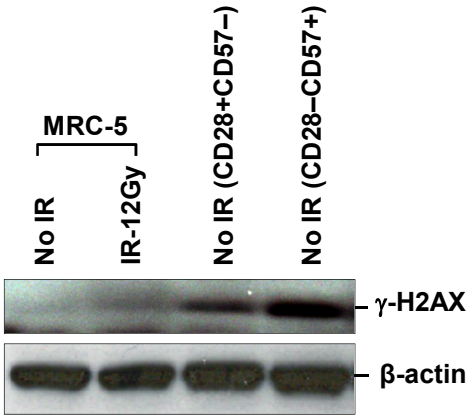

Supplemental Figure 4

Elevated expression of γ-H2AX in the late-differentiated $CD28^{-}CD57^{+}$ subset *in vivo*. Immunoblot analysis of γ-H2AX expression was performed in $CD28^{-}CD57^{+}$ and $CD28^{+}CD57^{-}$ subsets of $CD8^{+}$ T lymphocytes. Irradiated MRC-5 (normal human fibroblast), compared with unirradiated cells, was used as a positive control. IR, irradiated; No IR, unirradiated. β-actin was the loading control.

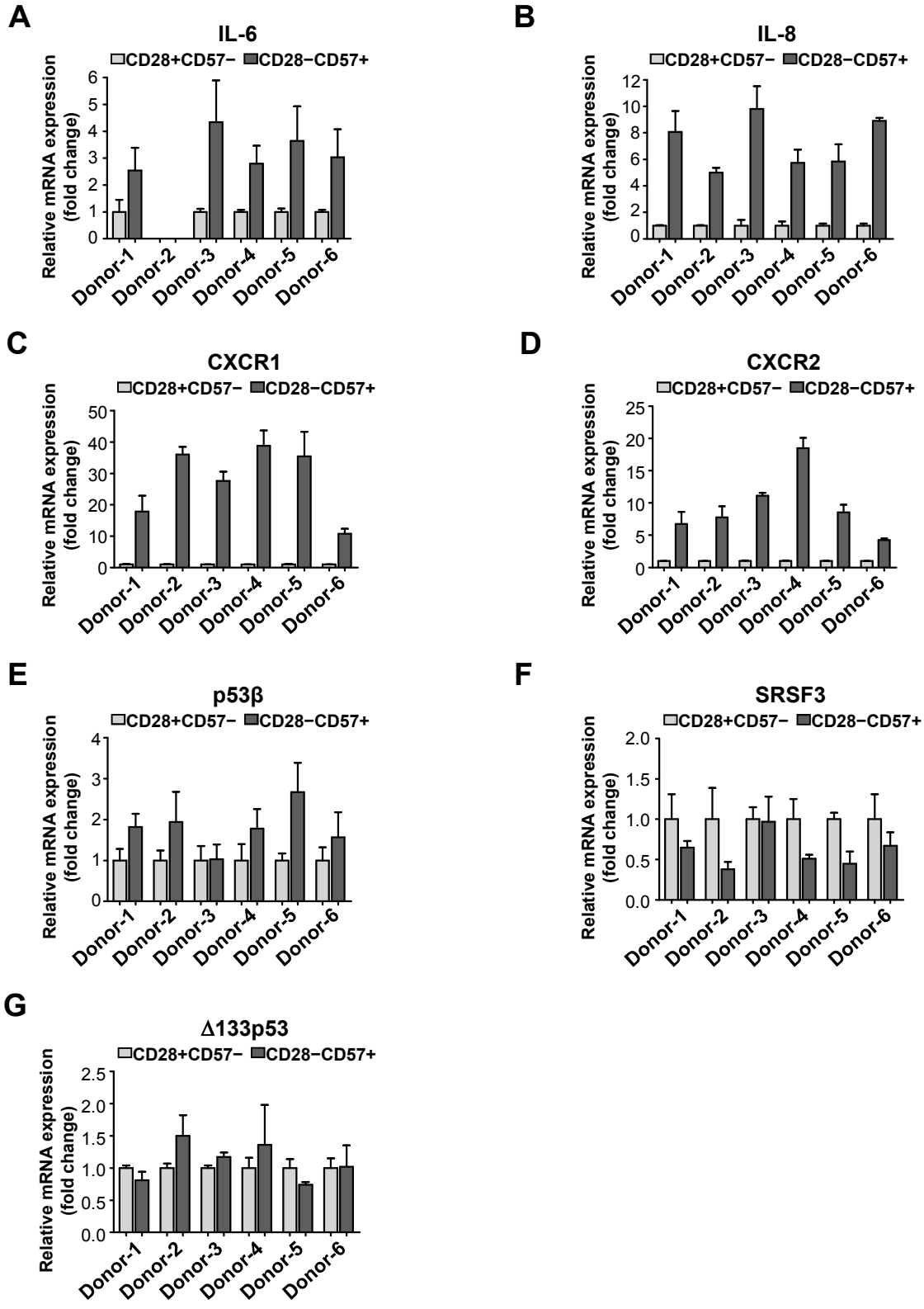

Supplemental Figure 5

CD28⁻CD57⁺ populations show increased expression of p53β and senescence-associated secretory phenotype (SASP) factors. Real-time qRT-PCR analyses for p53β and SASP-related genes were performed in the CD28⁺CD57⁻ and CD28⁻CD57⁺ populations of CD8⁺ T lymphocytes from six donors. Relative mRNA expression levels of IL-6 (**A**), IL-8 (**B**), CXCR1 (**C**), CXCR2 (**D**), p53β (**E**), SRSF3 (**F**) and Δ133p53 (**G**) in the CD28⁻CD57⁺ populations are shown as compared to CD28⁺CD57⁻ populations. β-2 microglobulin was used to normalize the data. Data are mean ± SD from triplicate assays.

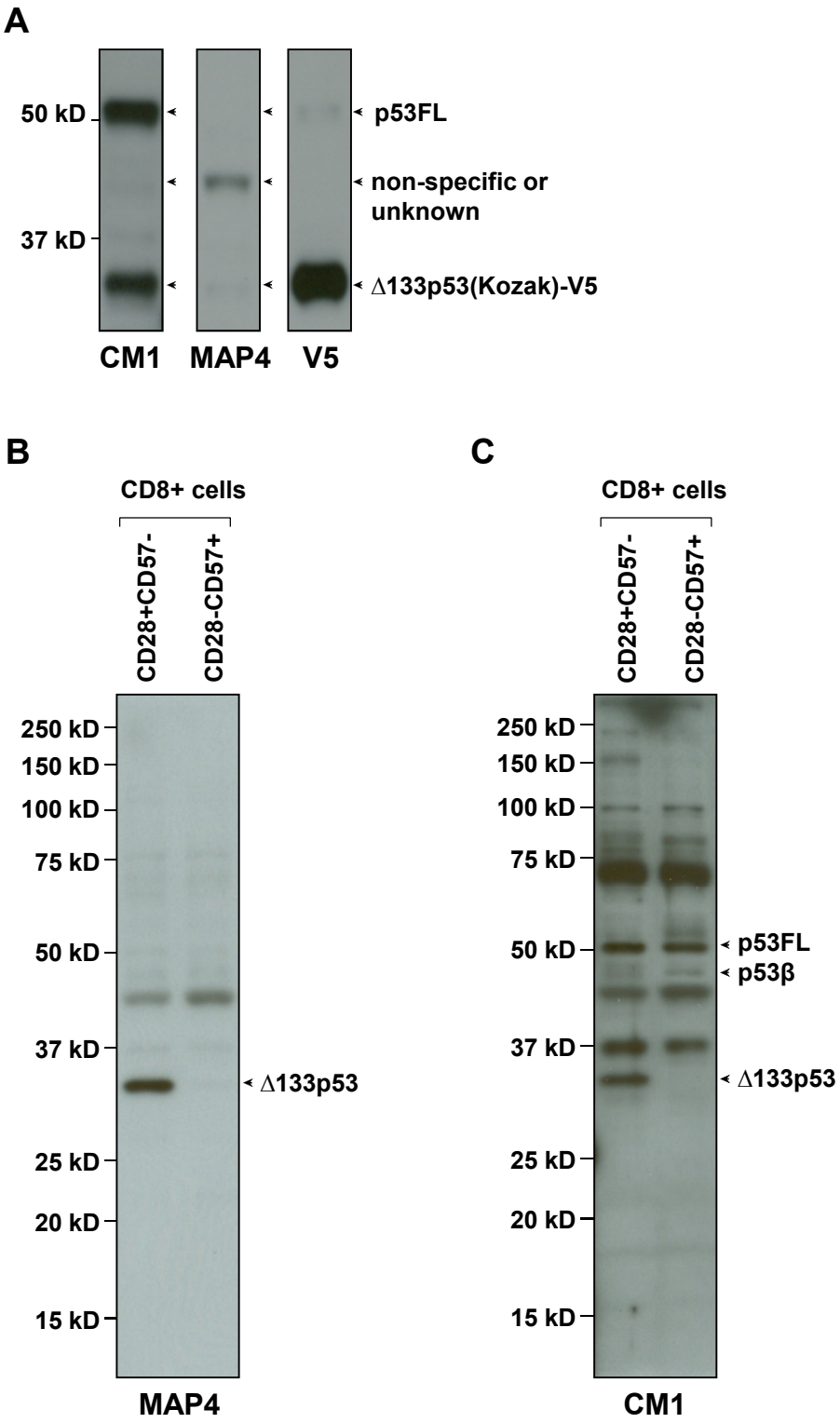

Supplemental Figure 6

Full immunoblot profiling of p53 isoforms. (**A**) Loss of MAP4 reactivity upon N-terminal modification of Δ133p53. Immunoblot of Δ133p53 with N-terminal Kozak modification (MGFCQLAKTC…, inserted amino acid underlined; Kozak M. Nucleic Acids Res. 1987, 15:8125-8148) and C-terminal V5-tag fusion expressed in MRC-5 fibroblasts. CM1, MAP4 and anti-V5 antibodies were used. MAP4 antibody does not recognize this modified version of Δ133p53, suggesting its specificity to the N-terminal sequence of Δ133p53. (**B** and **C**) Full immunoblot of $CD28^{+}CD57^{-}$ and $CD28^{-}CD57^{+}$ subsets of blood $CD8^{+}$ T lymphocytes (Donor-34) using antibodies MAP4 (**B**) and CM1 (**C**). Full-length p53 (p53FL), Δ133p53 and p53β are indicated.

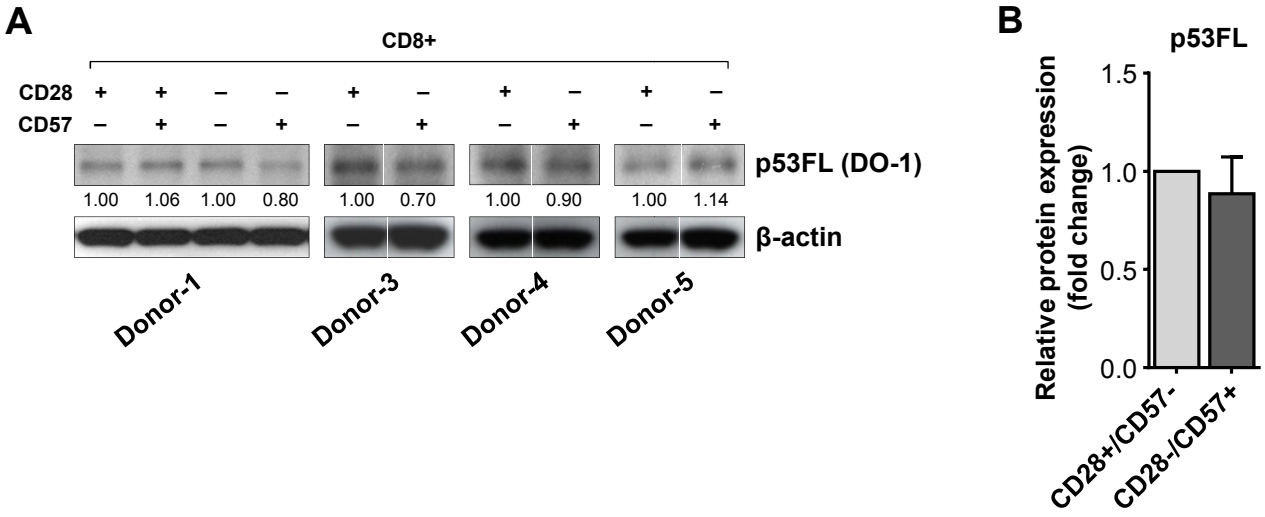

Supplemental Figure 7

Expression of full-length p53 (p53FL) in the $CD28^{+}CD57^{-}$ and $CD28^{-}CD57^{+}$ subset of $CD8^{+}$ T lymphocytes *in vivo*. (**A**) Immunoblot of CD28/CD57 quadrants of blood $CD8^{+}$ T lymphocytes showing p53FL protein. The lanes were run on the same gel but were non-contiguous (Donors 3-5). The DO-1 antibody detected p53FL. β-actin was the loading control. Densitometric values (normalized with β-actin and compared to the $CD28^{+}CD57^{-}$ subset) are shown below each lane. (**B**) Quantitative data summary of p53FL protein expression. Data are mean ± SD from four donors shown in **A**.

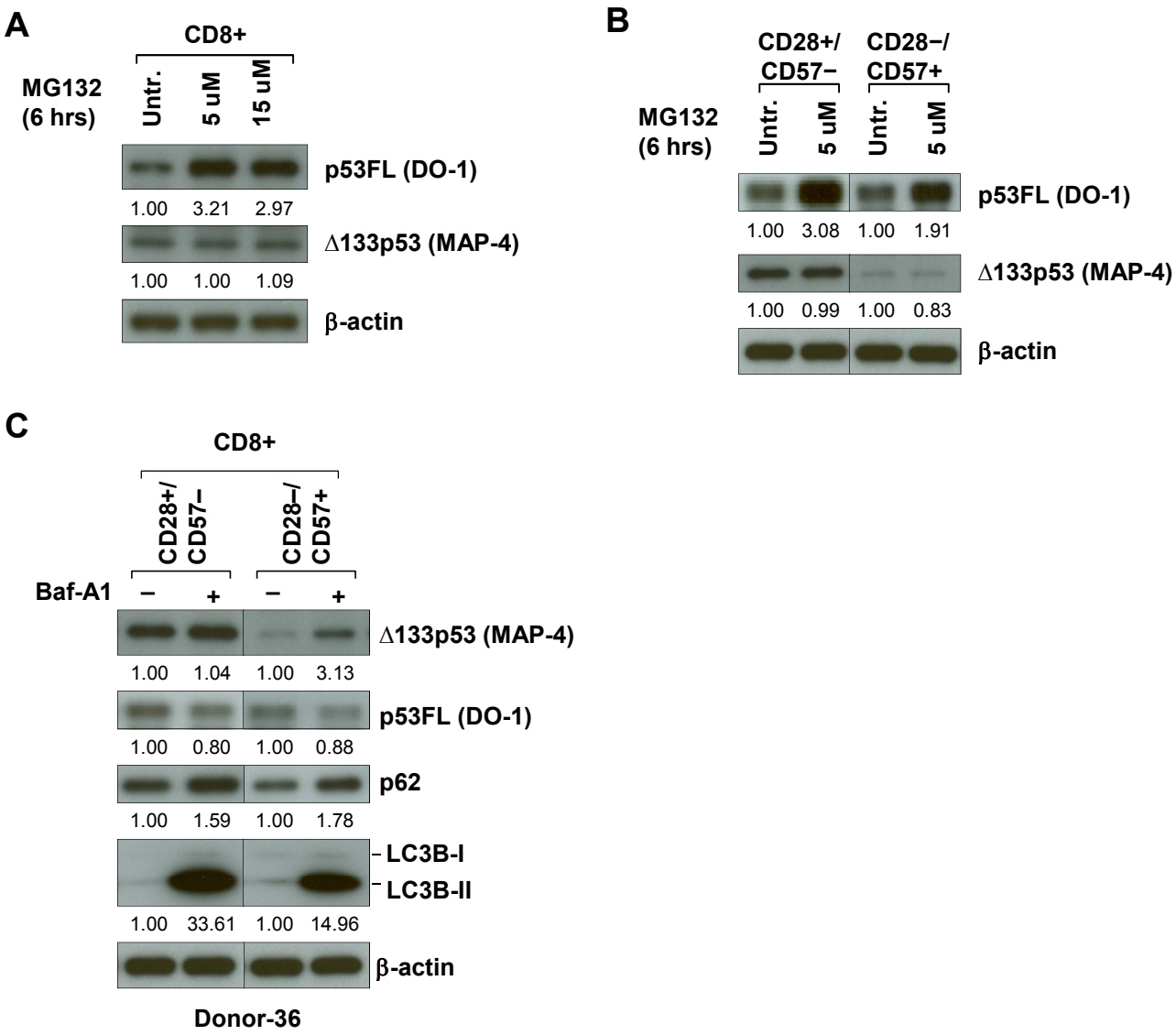

Supplemental Figure 8

Δ133p53 protein does not undergo proteasomal degradation. (**A**) Immunoblot of whole CD8$^+$ T lymphocytes treated with MG132 showing p53FL and Δ133p53 proteins (Donor-34). β-actin was the loading control. Densitometric values (normalized with β-actin and compared to untreated cells) are shown below each lane. (**B**) Immunoblot of the MG132 treated CD28$^+$CD57$^-$ and CD28$^-$CD57$^+$ subsets of CD8$^+$ T lymphocytes showing p53FL and Δ133p53 proteins (Donor-34). β-actin was the loading control. Densitometric values (as described in **A**) are shown below each lane. (**C**) Immunoblot of bafilomycin A1 (Baf A1, 100 nM for 6 h)-treated CD28$^+$CD57$^-$ and CD28$^-$CD57$^+$ subsets of blood CD8$^+$ T lymphocytes from donor-36. Δ133p53, p53FL, p62 and LC3B proteins were examined. Inhibition of autophagy was confirmed by increased amounts of p62 and LC3B-II. Densitometric values (compared to untreated cells) are shown below each lane.

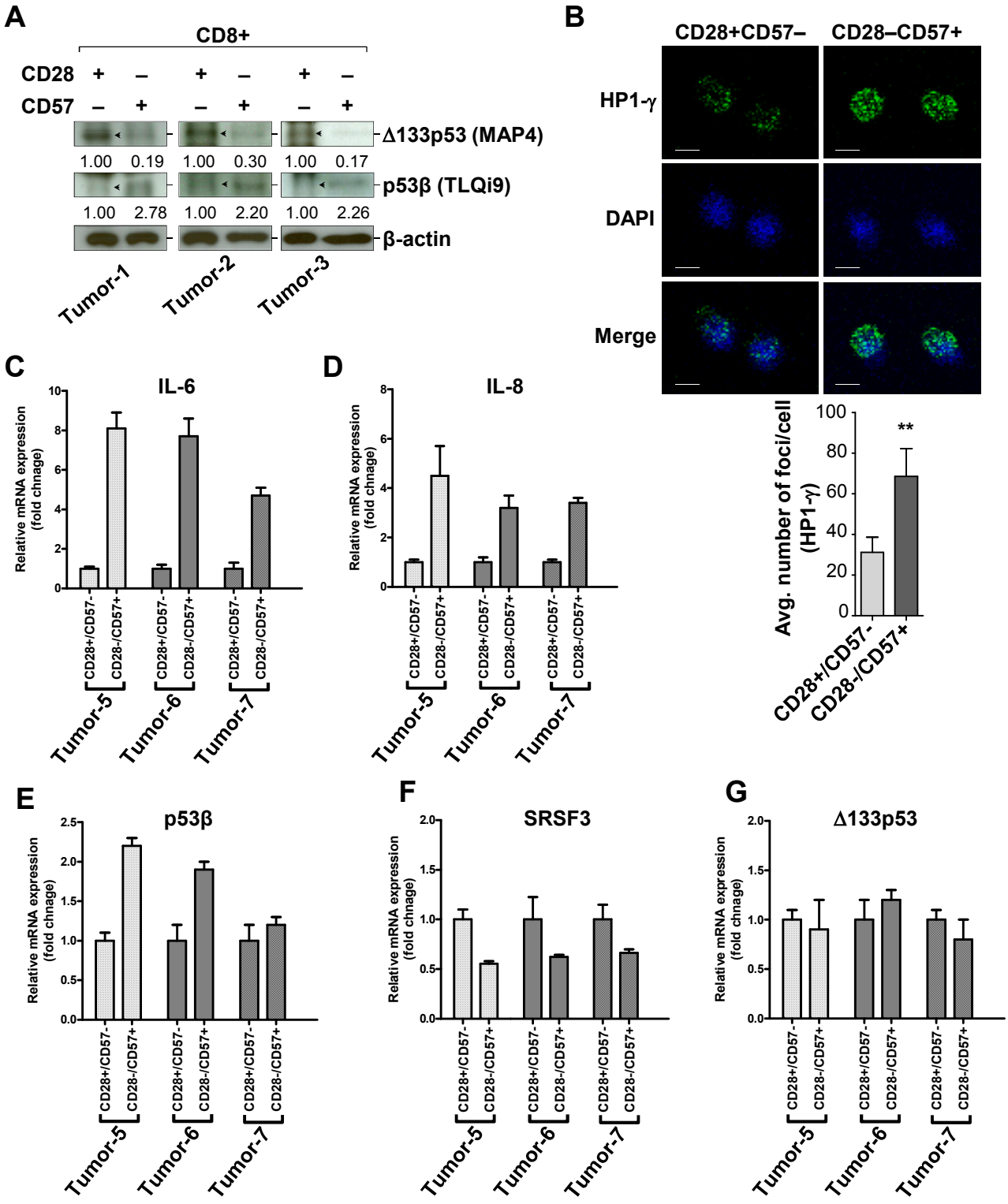

Supplemental Figure 9

Tumor-associated CD28⁻CD57⁺ subsets of CD8⁺ T lymphocytes show senescence phenotypes *in vivo*. (**A**) Immunoblot of CD28⁺CD57⁻ and CD28⁻CD57⁺ subsets of tumor-associated CD8⁺ T lymphocytes showing Δ133p53 and p53β proteins. Fewer cells (~3000 cells per subset) were used because of limited availability. Densitometric values (normalized with β-actin and compared to the CD28⁺CD57⁻ subset) are shown below each lane. (**B**) (upper) Representative images for HP1-γ foci by immunofluorescence staining in the CD28⁺CD57⁻ and CD28⁻CD57⁺ subsets (Tumor-4). Scale bars: 5 μm. (lower) Quantitative analysis of HP1-γ foci per cell. Data are mean ± SD from triplicate assays. (**C**-**G**) Quantitative RT-PCR analysis for the SASP factors IL-6 (C) and IL-8 (D), p53β (E), SRSF3 (F) and Δ133p53 (G) in the CD28⁺CD57⁻ and CD28⁻CD57⁺ subsets. β2-microglobulin (β2-M) was used for normalization. Data are mean (fold change) ± SD from 3 tumors (Tumors 5-7).

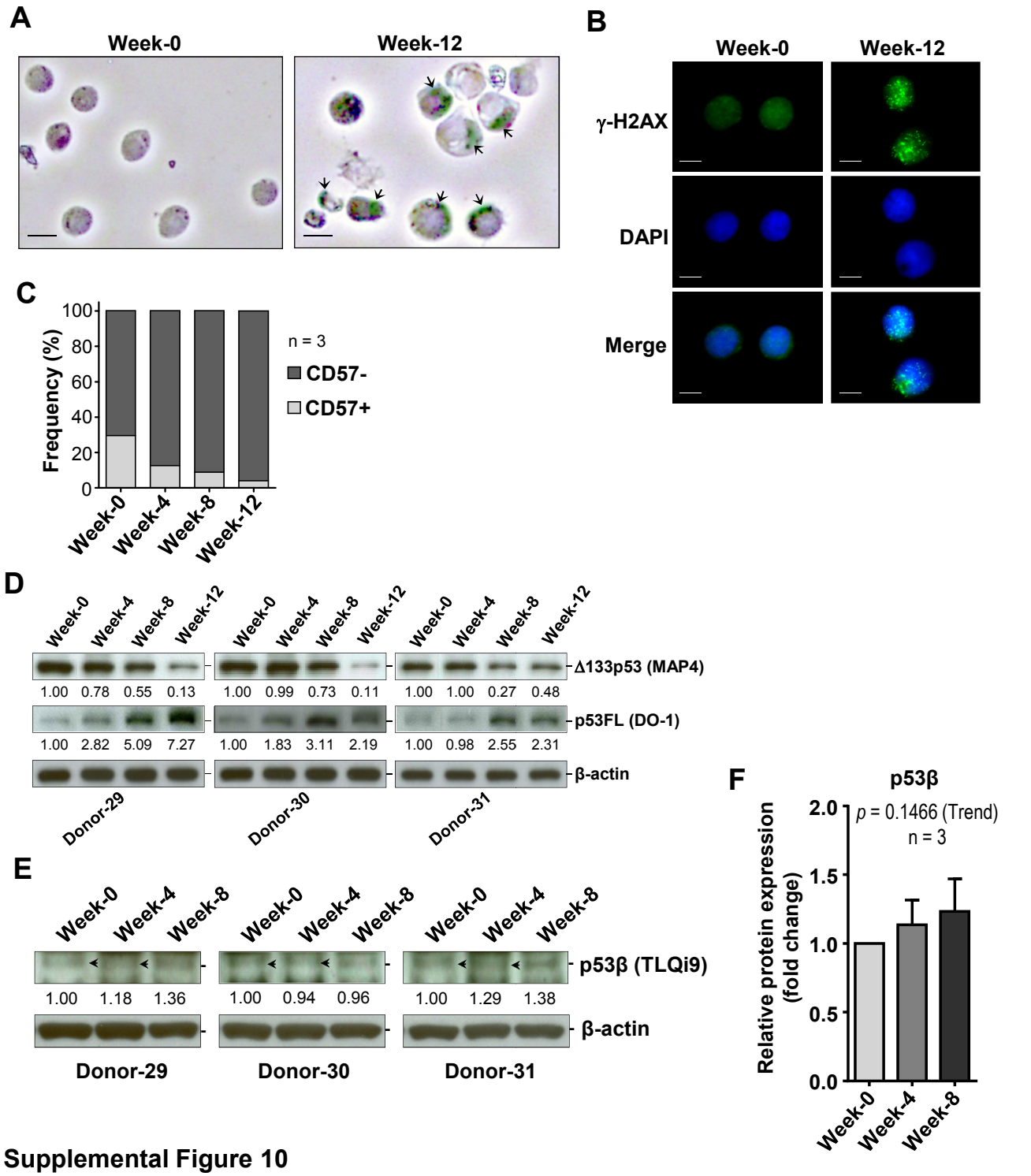

Supplemental Figure 10

CD8⁺ T lymphocytes from blood undergo replicative senescence *in vitro*. (**A**) Representative SA-β-gal staining of early-passage (Week-0) and late-passage (Week-12) CD8⁺ T lymphocytes (Donor-29). Cytoplasmic blue staining for SA-β-gal activities is marked by arrows. Scale bars: 10 μm. (**B**) Representative immunofluorescence staining of γ-H2AX at Week-0 and Week-12 (Donor-29). DAPI was used for nuclear staining. Scale bars: 5 μm. **(C)** Frequency of CD57⁺ and CD57⁻ subsets of the CD8⁺ T lymphocytes during in vitro culture. Data are the mean values from three donors (Donors 29-31). (**D**) Immunoblot analysis of Δ133p53 and full-length p53 (p53FL). β-actin was the loading control for normalization. Relative expression levels are shown below each lane. (**E**) Immunoblot analysis of p53β at Week-0, 4, and 8. Relative expression levels are shown below each lane. Protein samples at week-12 could not be included in this assay because of the limited protein amounts from fewer numbers of senescent cells. (**F**) Quantitative data summary of p53β protein expression. Linear trend analysis was performed and the p-value is shown. Data are mean ± SD from three donors shown in **E**.

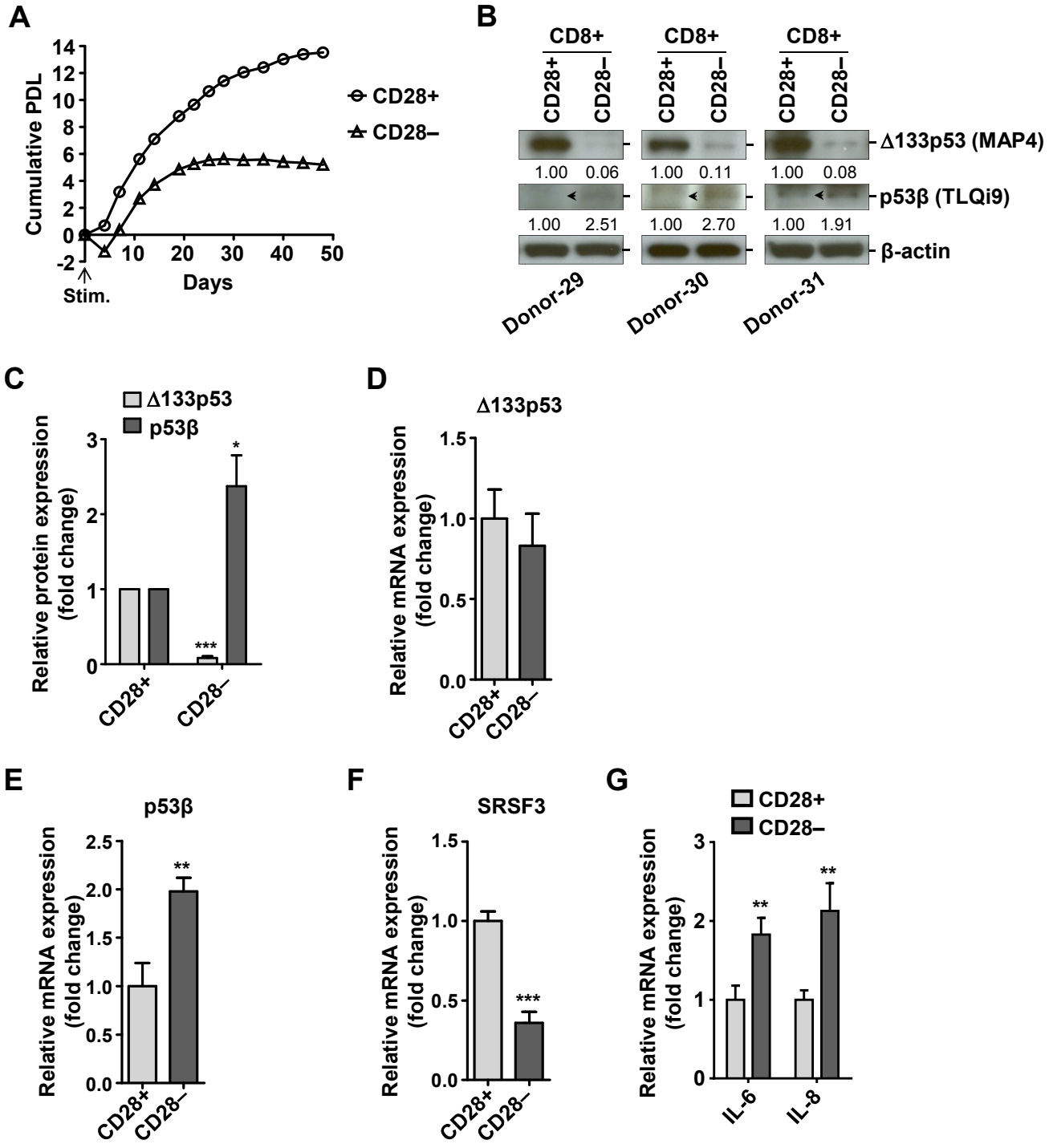

Supplemental Figure 11

Replicative potential and p53 isoform expression in $CD8^+CD28^+$ and $CD8^+CD28^-$ T lymphocytes isolated from blood. (**A**) Cumulative population doubling levels (PDL) of the FACS-sorted $CD28^+$ and $CD28^-$ populations of $CD8^+$ T lymphocytes after stimulation with anti-CD2/3/28 cocktail and rIL-2 (Donor-29). (**B**) Δ133p53 and p53β protein levels were examined by immunoblot analysis in $CD28^+$ and $CD28^-$ populations of $CD8^+$ T lymphocytes (Donors 29-31). The MAP4 and TLQi9 antibodies detected Δ133p53 and p53β, respectively. β-actin was the loading control. Densitometric values (normalized with β-actin and compared to the $CD28^+$ population) are shown below each lane. (**C**) Quantitative data summary of Δ133p53 and p53β expression in $CD28^+$ and $CD28^-$ subsets. Data are mean ± SD from three donors shown in **B**. (**D**-**G**) Quantitative RT-PCR analysis for Δ133p53 (D), p53β (E), SRSF3 (F) and the SASP factors IL-6 and IL-8 (G) in $CD28^+$ and $CD28^-$ subsets. β2-M was used for normalization. Data are mean (fold change) ± SD from three donors (Donors 29-31). $^*P < 0.05$; $^{**}P < 0.01$; $^{***}P < 0.001$.

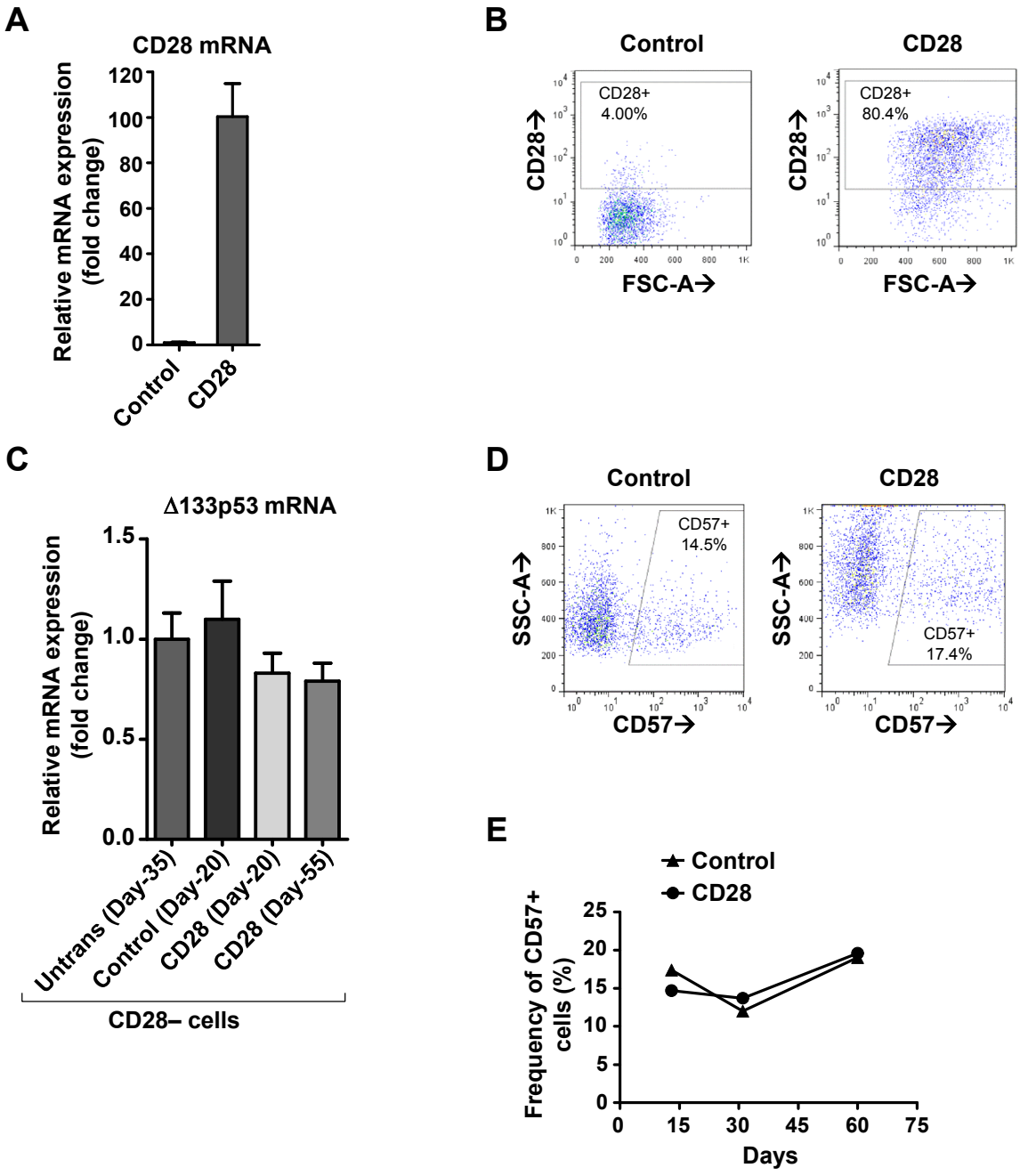

Supplemental Figure 12

Reconstitution of CD28 expression in blood $CD8^{+}CD28^{-}$ T lymphocytes. (**A**) Quantitative RT-PCR analysis of CD28 mRNA at day-20 post-selection confirmed reconstitution of CD28 expression (Donor-29). β2-M was used for normalization. Data are mean ± SD from triplicate assays. (**B**) Representative dot plots for CD28 expression by flow cytometry at day-13 post-selection (Donor-29). CD28-transduced cells showed >80% of $CD28^{+}$ cells, while empty vector-transduced cells (Control) were mostly $CD28^{-}$. (**C**) Quantitative RT-PCR analysis for Δ133p53 mRNA in CD28-transduced $CD28^{-}$ cells (Donor-29). Empty vector-transduced (Control) and untransduced (Untrans) cells were used as controls. β2-M was used for normalization. Data are mean ± SD from triplicate assays. (**D**) Representative dot plots for CD57 expression by flow cytometry at day-13 (Donor-29). CD57 expression remained unchanged in the CD28-transduced cells compared to the control cells. (**E**) Quantitative summary of $CD57^{+}$ cells in CD28-transduced and control cells at day-13 (shown in **D**), day-31 and day-60 (Donor-29).

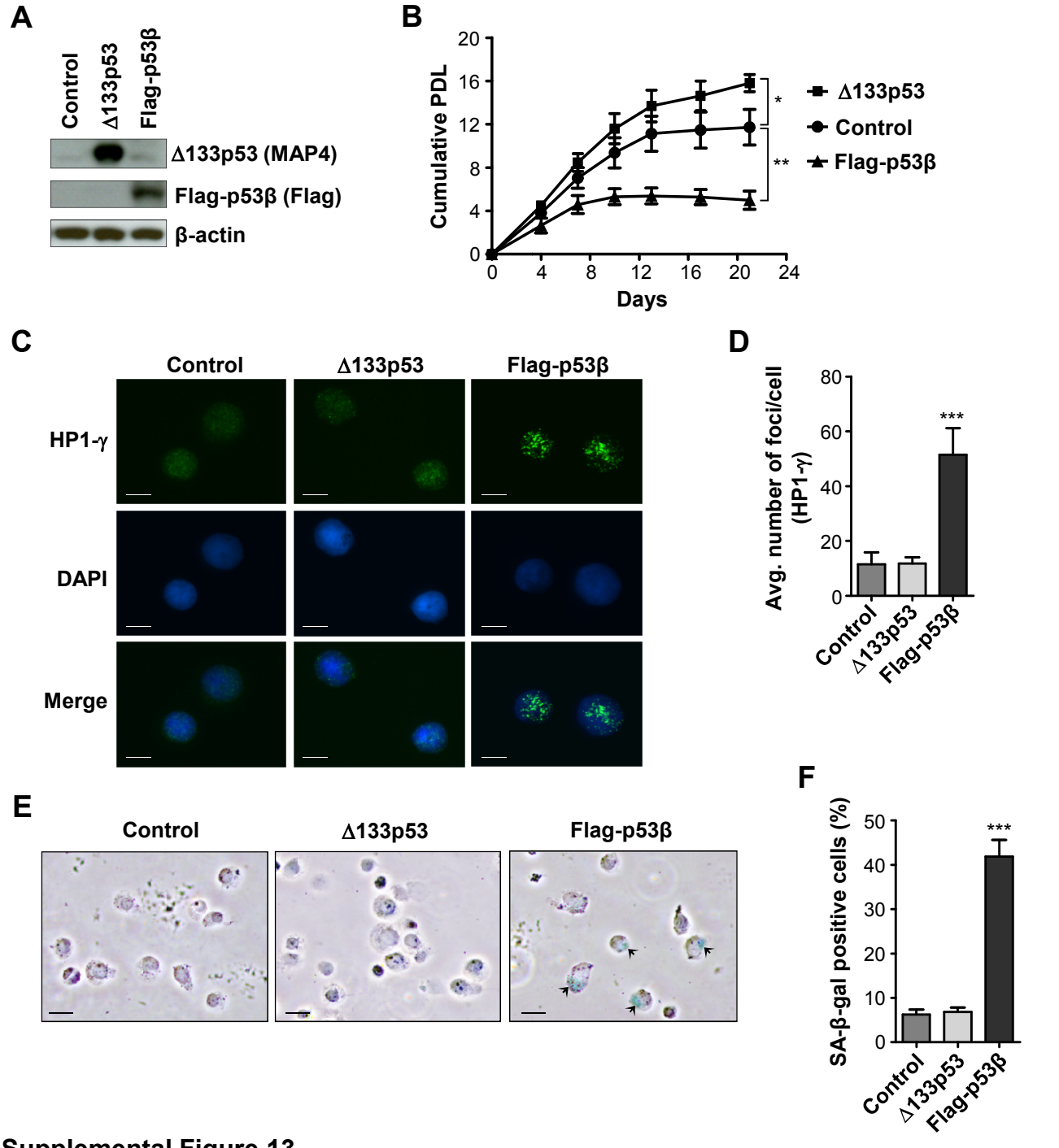

Supplemental Figure 13

Overexpression of Δ133p53 and p53β delays and induces, respectively, replicative senescence in whole CD8⁺ T lymphocytes. FACS-sorted CD8⁺ T lymphocytes were stimulated at day-0 and transduced with a lentiviral overexpressing vector for Δ133p53 or Flag-tagged p53β. Empty lentiviral vector was used as a control. Selection with blasticidin started at day-5 and continued for 10-12 days. Selected cells were expanded in culture until they stopped proliferating. (**A**) Δ133p53 and p53β levels were examined by immunoblot analysis at day-7 post-selection (Donor-10). The MAP4 and Flag antibodies detected Δ133p53 and Flag-p53β, respectively. β-actin was the loading control. (**B**) Cumulative PDL of the post-selected cells. Data are mean ± SD from three donors (Donors 10-12). *$P < 0.05$; **$P < 0.01$. (**C**) Representative images for HP1-γ foci by immunofluorescence staining at day-21 post-selection (Donor-10). Nuclei were counterstained with DAPI. Scale bars: 5 μm. (**D**) Quantitative analysis of HP1-γ foci per cell. Data are mean ± SD from three donors (Donors 10-12). ***$P < 0.001$. (**E**) Representative images for SA-β-gal activity at day-21 post-selection (Donor-10). Arrows in Flag-p53β overexpressing cells indicate SA-β-gal positive cells. Scale bars: 10 μm. (**F**) Quantitative analysis of SA-β-gal positive cells. Data are mean ± SD from three donors (Donors 10-12). ***$P < 0.001$.

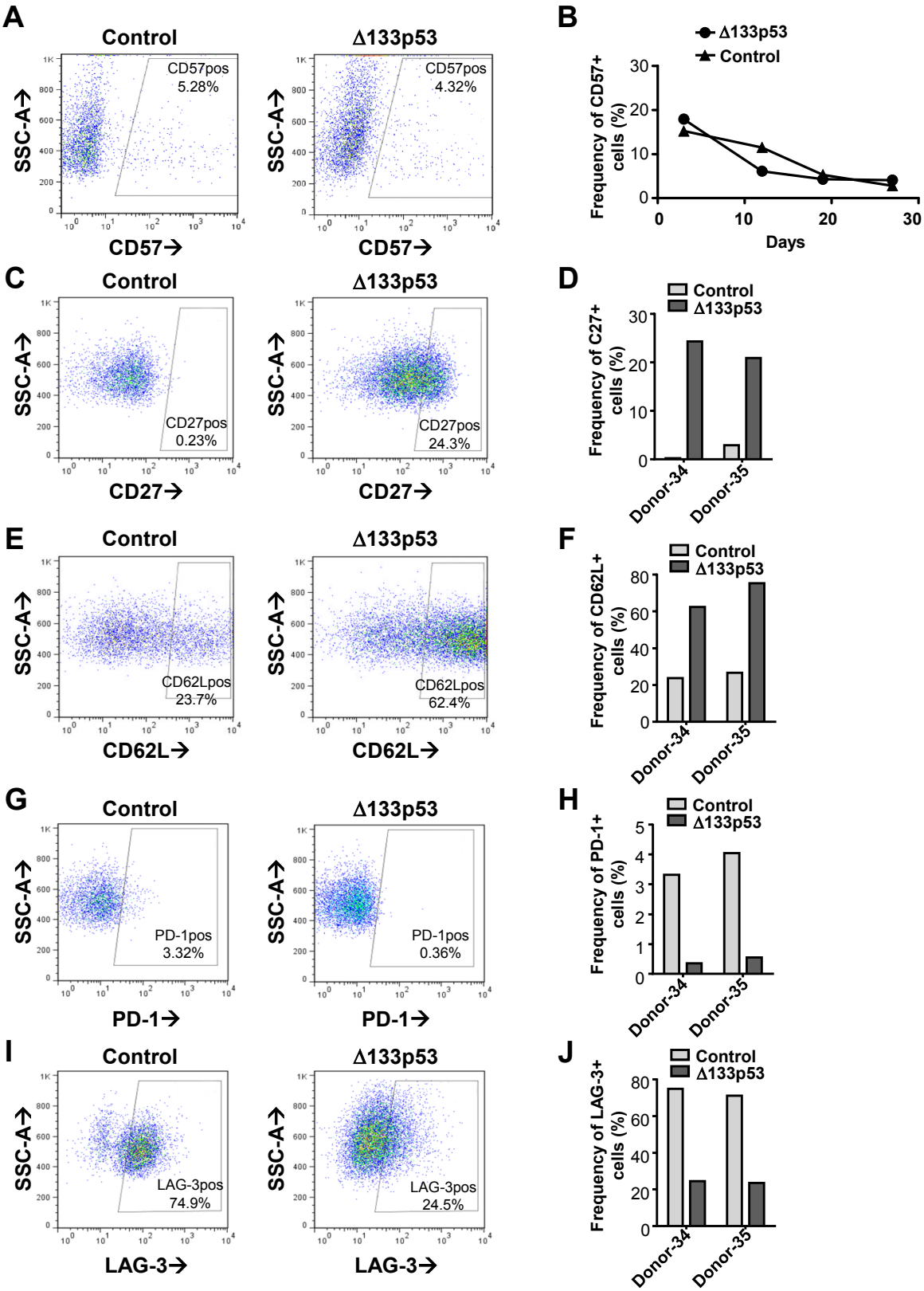

Supplemental Figure 14

Rescued senescence phenotypes in the CD8$^+$CD28$^-$ T lymphocytes with restoration of Δ133p53 expression. (**A**) Representative dot plots for CD57 expression by flow cytometry in empty vector- (Control) or Δ133p53-transduced CD28$^-$ cells at day-19 post-selection by blasticidin (Donor-29). (**B**) Quantitative summary of CD57$^+$ cells in empty vector- (Control) or Δ133p53-transduced CD28$^-$ cells at day-3, day-12, day-19 (shown in **A**) and day-27 (Donor-29). (**C**) Representative dot plots for CD27 expression at day-25 (Donor-34). (**D**) Frequency of CD27$^+$ cells at day-25 (Donors 34 and 35). (**E**) Representative dot plots for CD62L expression at day-25 (Donor-34). (**F**) Frequency of CD27$^+$ cells at day-25 (Donors 34 and 35). (**G**) Representative dot plots for PD-1 expression at day-25 (Donor-34). (**H**) Frequency of PD-1$^+$ cells at day-25 (Donors 34 and 35). (**I**) Representative dot plots for LAG-3 expression at day-25 (Donor-34). (**J**) Frequency of LAG-3$^+$ cells at day-25 (Donors 34 and 35).

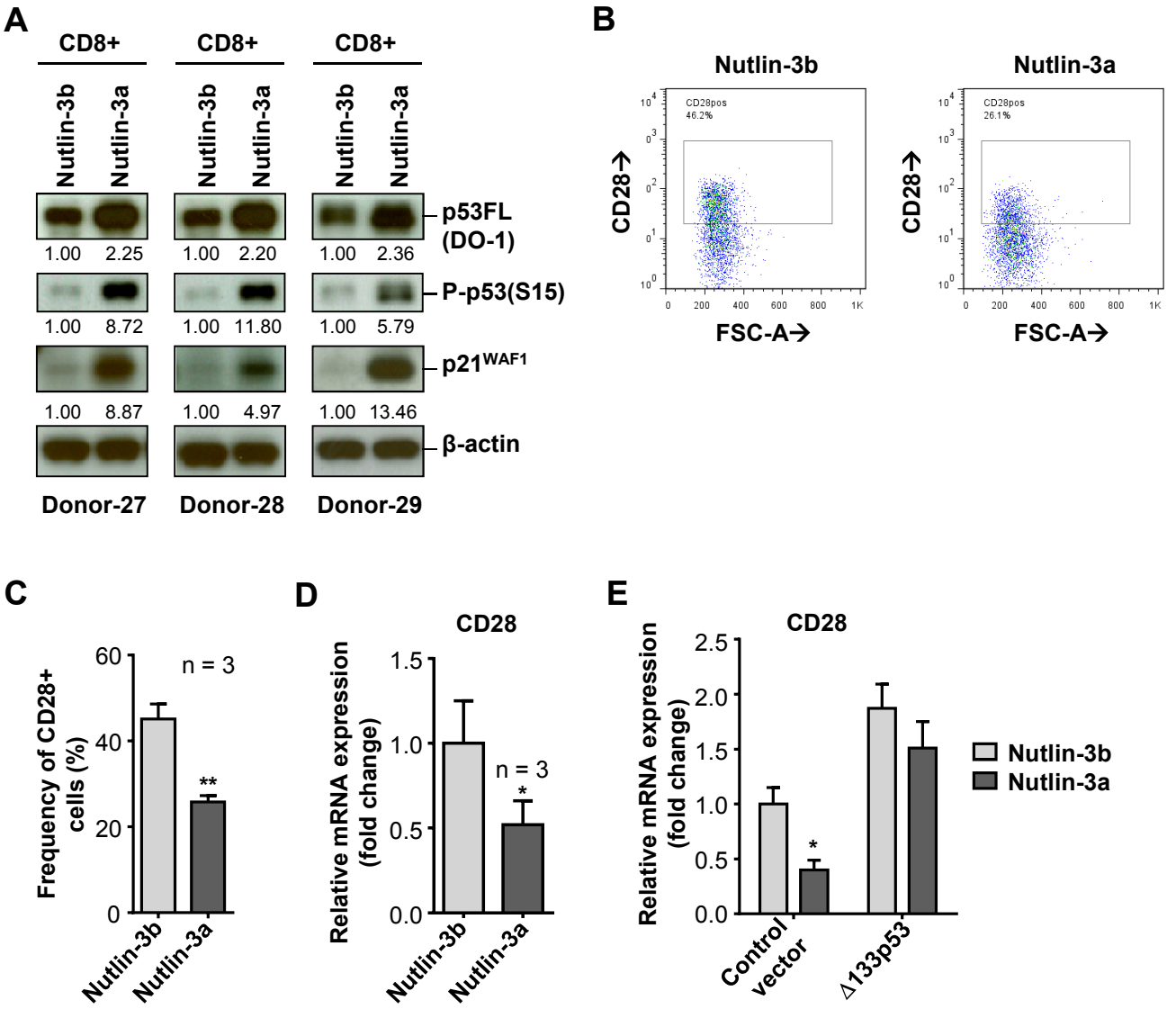

Supplemental Figure 15

Δ133p53 counteracts nutlin-3a-induced repression of CD28 mRNA. (**A**) Immunoblot of nutlin-treated (at 5 uM for 48 h) whole CD8⁺ T lymphocytes from donors 27-29 showing full-length p53 (p53FL), phosphorylated p53 [P-p53(S15)] and $p21^{WAF1}$. Nutlin-3a is the active enantiomer of nutlin-3, and nutlin-3b is the inactive enantiomer as a control. β-actin was the loading control. Densitometric values (compared to nutlin-3b treated cells) are shown below each lane. (**B**) Representative dot plots for CD28 expression by flow cytometry in nutlin-3b and nutlin-3a treated CD8⁺ T lymphocytes (Donor-27). (**C**) Quantitative summary of CD28⁺ cells in nutlin-3b and nutlin-3a treated cells. Data are mean ± SD from three donors (Donors 27-29). (**D**) Quantitative RT-PCR analysis for CD28 mRNA expression. β2-M was used for normalization. Data are mean (fold change) ± SD from three donors (Donors 27-29). **(E)** Quantitative RT-PCR analysis for CD28 mRNA expression in the Δ133p53-overexpressing CD8⁺ T lymphocytes after nutlin treatment (Donor-36). β2-M was used for normalization. Data are mean (fold change compared to control nutlin-3b) ± SD from triplicate assays. **P* < 0.05; ***P* < 0.01.

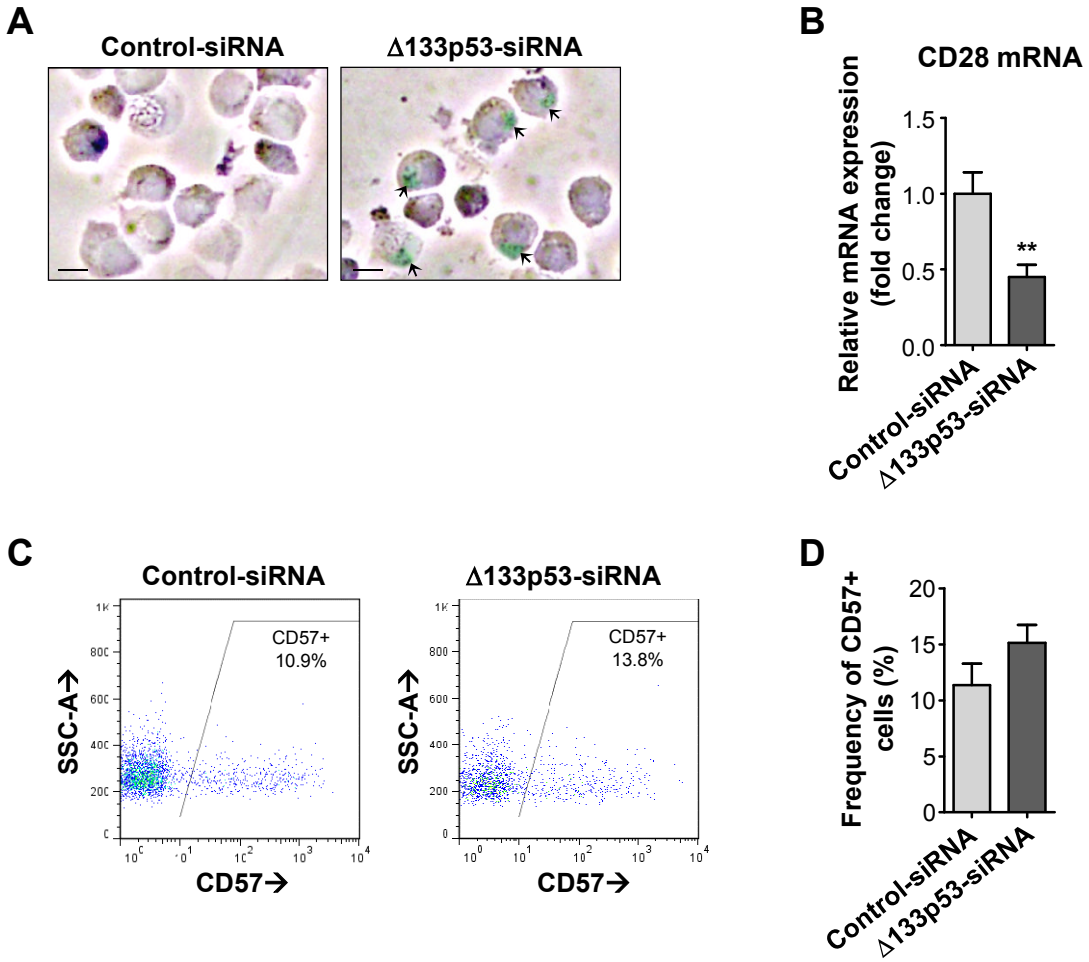

Supplemental Figure 16

Knockdown of Δ133p53 expression induces cellular senescence in $CD8^+CD28^+$ T lymphocytes. (**A**) Representative images for SA-β-gal activity after fifth nucleofection at day-18 (Donor-30). Arrows in the Δ133p53-siRNA nucleofected cells indicate SA-β-gal positive cells. Scale bars: 5 μm. (**B**) Quantitative RT-PCR analysis for CD28 mRNA at day-7. β2-M was used for normalization. Data are mean ± SD from three donors (Donors 29-31). (**C**) Representative dot plots for CD57 expression by flow cytometry in control siRNA- and Δ133p53 siRNA-nucleofected cells at day-18 (Donor-30). (**D**) Quantitative summary of $CD57^+$ cells at day-18. Data are mean ± SD from three donors (Donors 29-31). No significant difference was observed ($P = 0.1779$). $^{**}P < 0.01$.

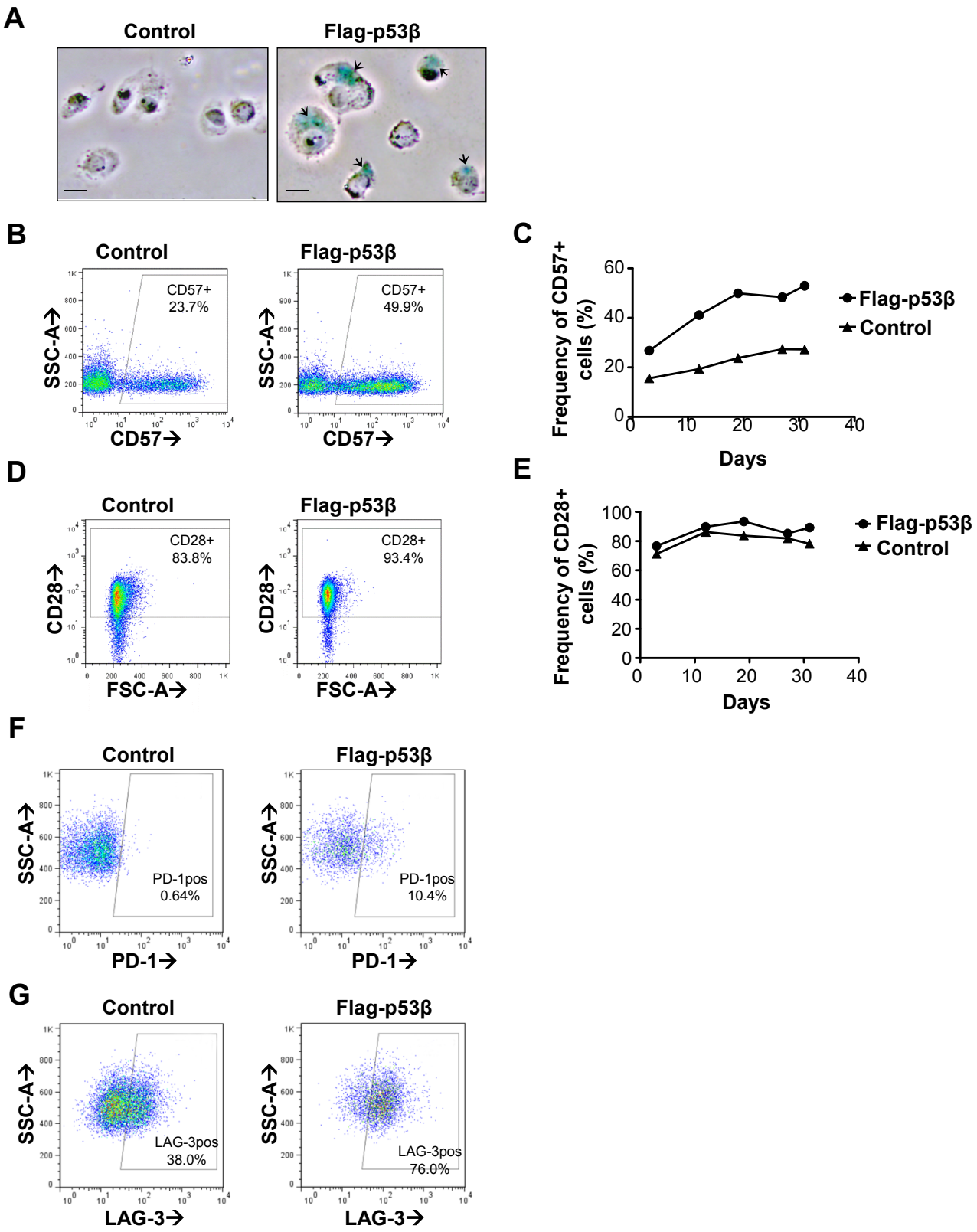

Supplemental Figure 17

p53β overexpression induces cellular senescence in CD8⁺CD28⁺ T lymphocytes. (**A**) Representative images for SA-β-gal activity in the empty vector- (Control) or Flag-tagged p53β-transduced CD28⁺ cells at day-19 (Donor-29). Arrows in the Flag-tagged p53β-transduced cells indicate SA-β-gal positive cells. Scale bars: 5 μm. (**B**) Representative dot plots for CD57 expression by flow cytometry at day-19 (Donor-29). (**C**) Frequency of CD57⁺ cells at day-3, day-12, day-19 (shown in **B**), day-27 and day-31 (Donor-29). (**D**) Representative dot plots for CD28 expression by flow cytometry at day-19 (Donor-29). (**E**) Frequency of CD28⁺ cells at day-3, day-12, day-19 (shown in **D**), day-27 and day-31. (**F-G**) Representative dot plots for PD-1 (F) and LAG-3 (G) expression by flow cytometry in empty vector- (Control) or Flag-p53β-transduced CD28⁺ cells at day-26 post-selection by blasticidin (Donor-32).

Supplemental Table 1

Information of blood bank donors and frequency of CD28/CD57 expressing fractions of CD8+ T lymphocytes

Donor	Age	Gender	Race	[CD28+CD57-]	[CD28+CD57+]	[CD28-CD57-]	[CD28-CD57+]
Donor-1	62	Male	Caucasian	33	16	19	32
Donor-2	65	Male	Caucasian	36	8	12	44
Donor-3	54	Male	Caucasian	23	6	33	38
Donor-4	23	Male	African American	72	7	8	13
Donor-5	24	Female	African American	42	9	25	23
Donor-6	54	Female	Caucasian	37	11	28	24
Donor-7	60	Male	African American	32	7	24	37
Donor-8	50	Male	Caucasian	49	5	26	20
Donor-9	63	Female	Caucasian	25	7	20	47
Donor-10	56	Male	Caucasian	49	2	22	28
Donor-11	46	Male	Caucasian	41	14	6	40
Donor-12	32	Male	Hispanic*	51	20	9	20
Donor-13	21	Male	Caucasian	62	10	5	24
Donor-14	34	Male	Caucasian	41	20	6	33
Donor-15	41	Male	Hispanic*	47	22	6	25
Donor-16	27	Male	Caucasian	48	13	4	36
Donor-17	32	Male	Caucasian	50	19	13	18
Donor-18	21	Male	Caucasian	77	7	3	12
Donor-19	25	Female	Caucasian	51	7	9	33
Donor-20	26	Female	Caucasian	83	4	8	5
Donor-21	35	Male	African American	61	7	11	21
Donor-22	33	Male	African American	63	9	4	24
Donor-23	32	Male	African American	72	3	6	19
Donor-24	47	Male	Caucasian	26	2	56	16
Donor-25	74	Male	African American	9	5	11	75
Donor-26	64	Male	Caucasian	31	11	17	41
Donor-27	35	Male	Caucasian	58	12	8	22
Donor-28	43	Female	African American	45	16	5	33
Donor-29	27	Female	African American	65	6	20	9
Donor-30	52	Female	Caucasian	39	8	19	34
Donor-31	34	Male	African American	58	14	11	18
Donor-32	48	Female	African American	33	12	16	39
Donor-33	31	Female	Caucasian	61	7	9	22
Donor-34	42	Male	Hispanic*	40	3	26	32
Donor-35	55	Male	Caucasian	30	11	10	49
Donor-36	45	Female	Caucasian	33	15	13	40

*** racial status among those with a 'Hispanic' ethnicity is unknown**

Supplemental Table 2

Information of lung cancer samples and frequency of CD28/CD57 expressing fractions of CD8+ T lymphocytes.

Tumor	Age	Gender	Histology	[CD28+CD57-]	[CD28+CD57+]	[CD28-CD57-]	[CD28-CD57+]
Tumor-1	78	Female	Adeno	57	7	26	10
Tumor-2	85	Male	Adeno	62	4	25	9
Tumor-3	75	Male	Squamous	84	4	10	2
Tumor-4	78	Female	Adeno	43	8	26	22
Tumor-5	65	Female	Adeno	54	9	28	9
Tumor-6	70	Female	Squamous	56	10	28	6
Tumor-7	75	Female	Adeno	66	13	19	3

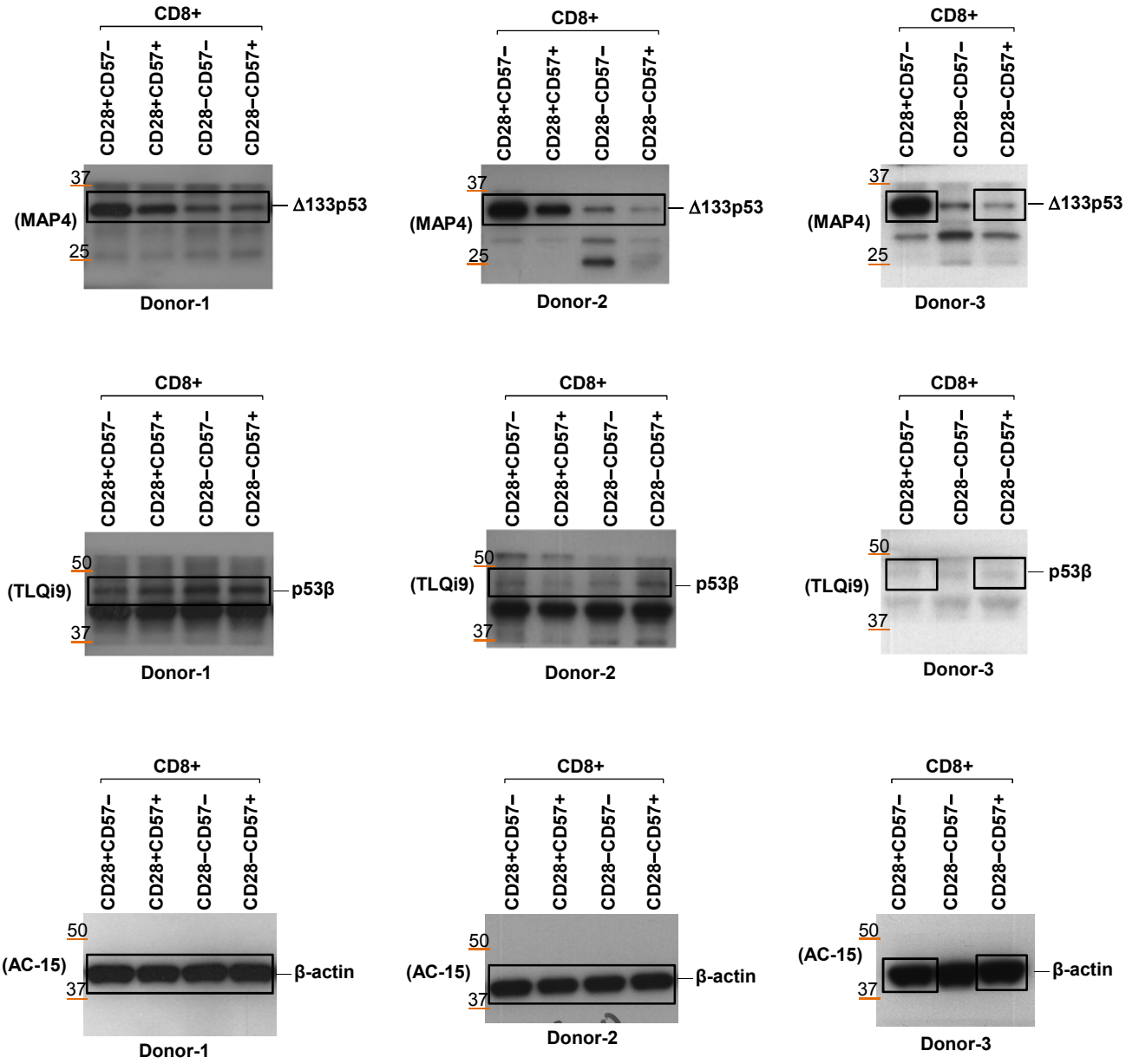

Full scan of immunoblots for Figure 2A (Donors 1-3)

The rectangular areas of the blots were put together and shown in Figure 2A (Donors 1-3) as the results of Δ133p53 and p53β protein levels using MAP4 and TLQi9 antibodies, respectively. AC-15 antibody was used to detect β-actin for the loading control. The cell subsets loaded were indicated for each lane .

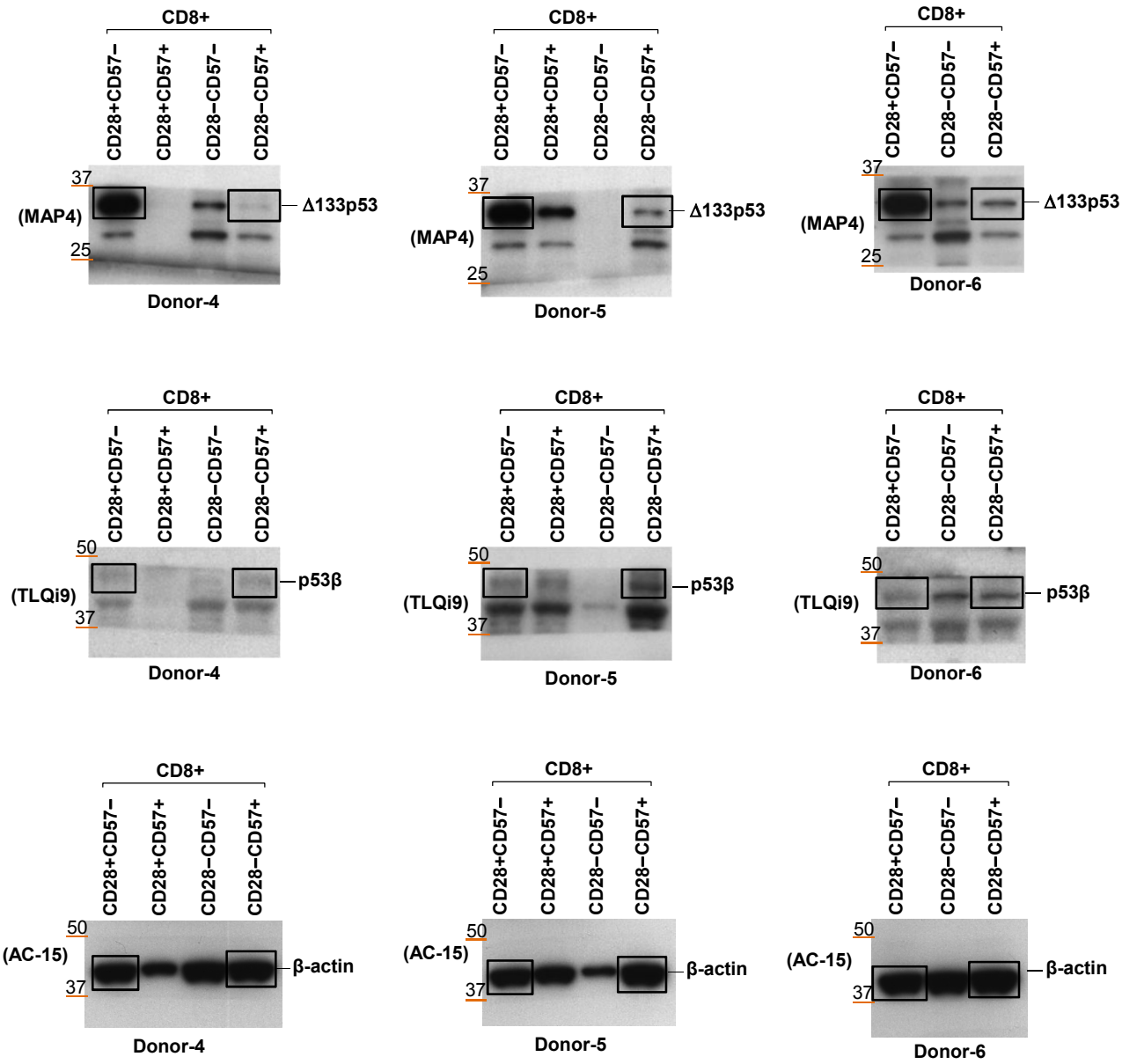

Full scan of immunoblots for Figure 2A (Donors 4-6)

The rectangular areas of the blots were put together and shown in Figure 2A (Donors 4-6) as the results of Δ133p53 and p53β protein levels using MAP4 and TLQi9 antibodies, respectively. AC-15 antibody was used to detect β-actin for the loading control. The cell subsets loaded were indicated for each lane .

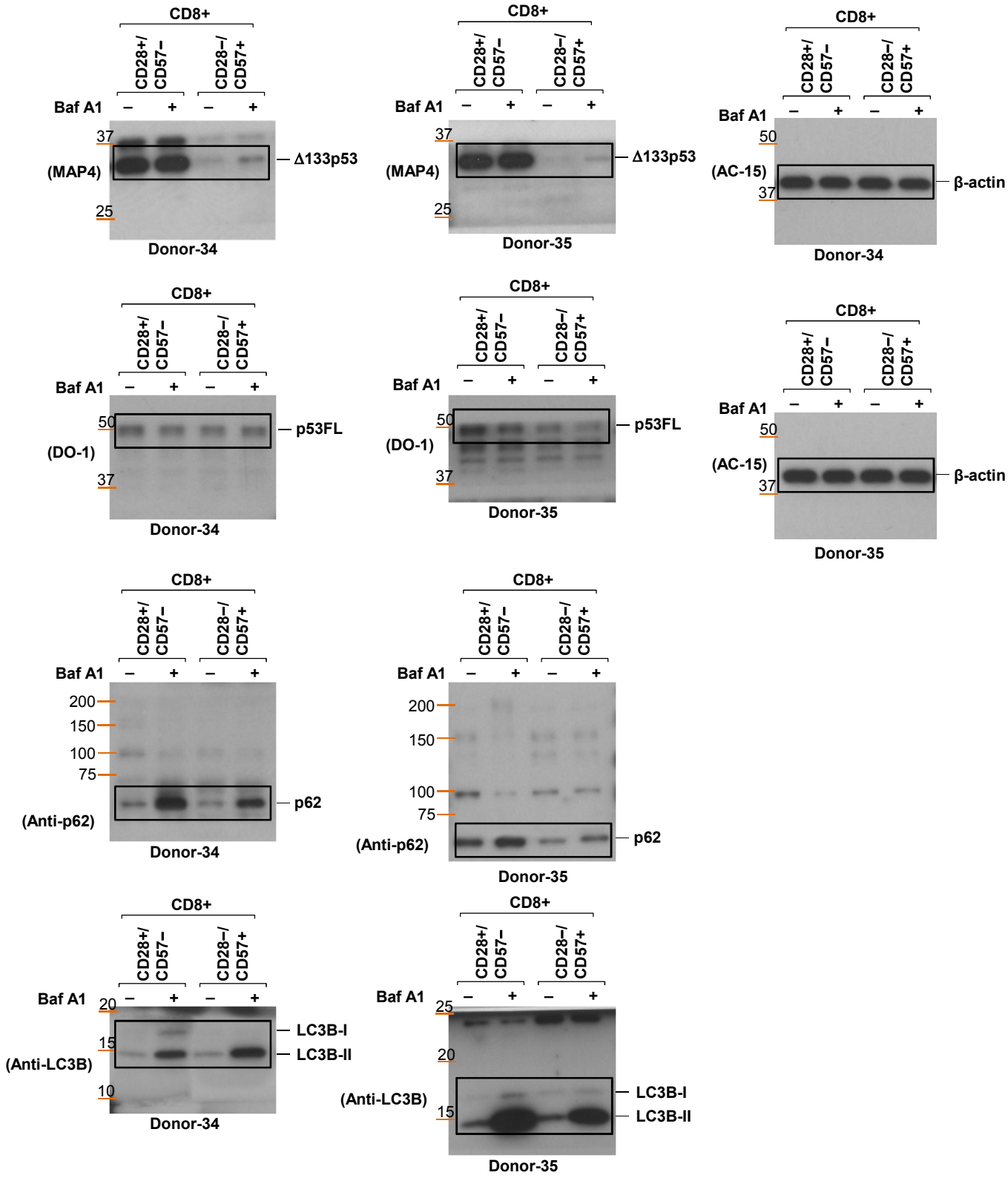

Full scan of immunoblots for Figure 2F

The rectangular areas of the blots were shown in Figure 2F as the results of Δ133p53, full-length p53 (p53FL), p62 and LC3B protein levels using MAP4, DO-1, anti-p62 and antiLC3B antibodies, respectively. AC-15 antibody was used to detect β-actin for the loading control. The cell subsets treated with bafilomycin A1 and untreated were indicated.

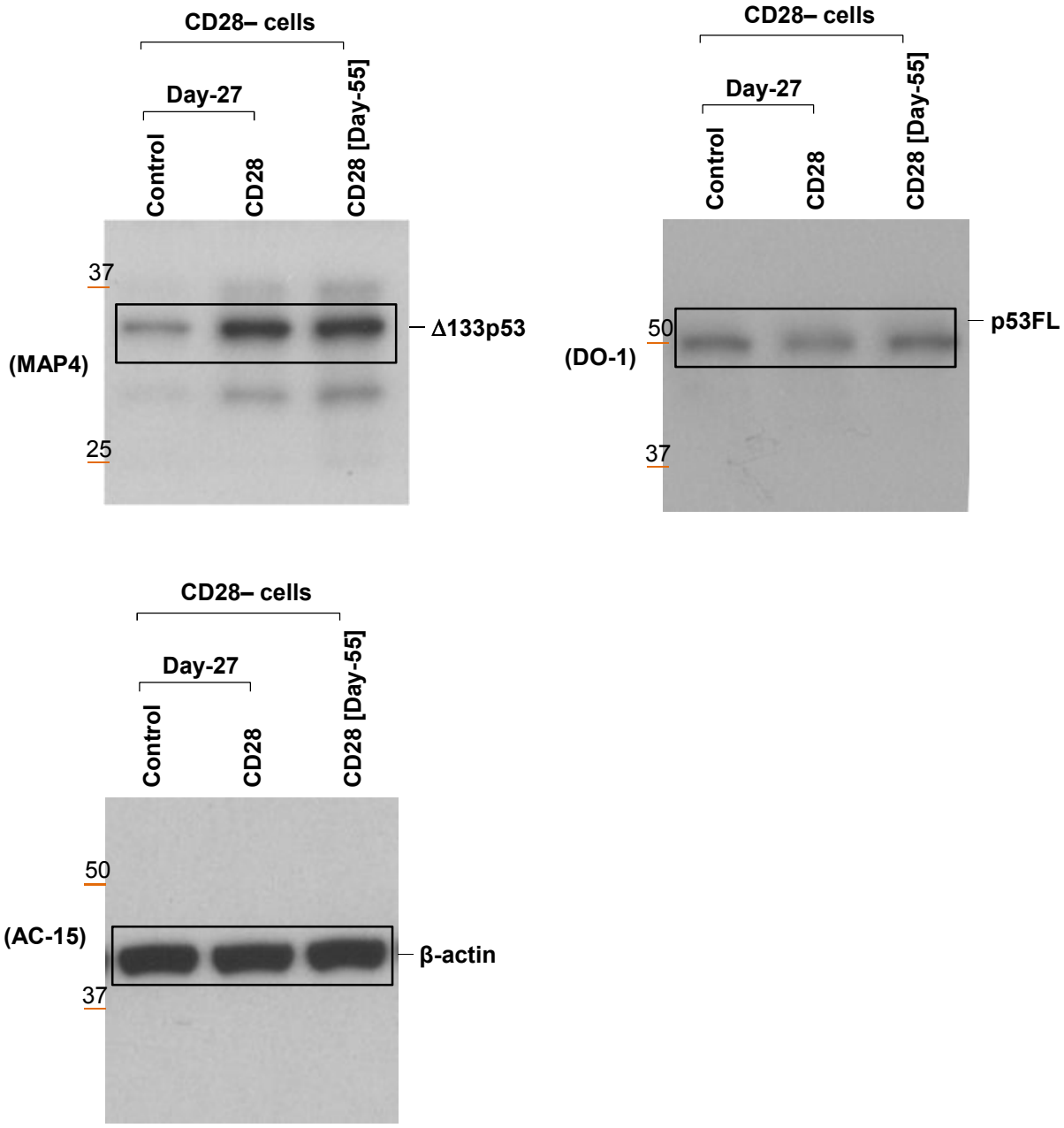

Full scan of immunoblots for Figure 4B

The rectangular areas of the blots were shown in Figure 4B as the results of Δ133p53, full-length p53 (p53FL) protein levels using MAP4 and DO-1 antibodies, respectively. AC-15 antibody was used to detect β-actin for the loading control.

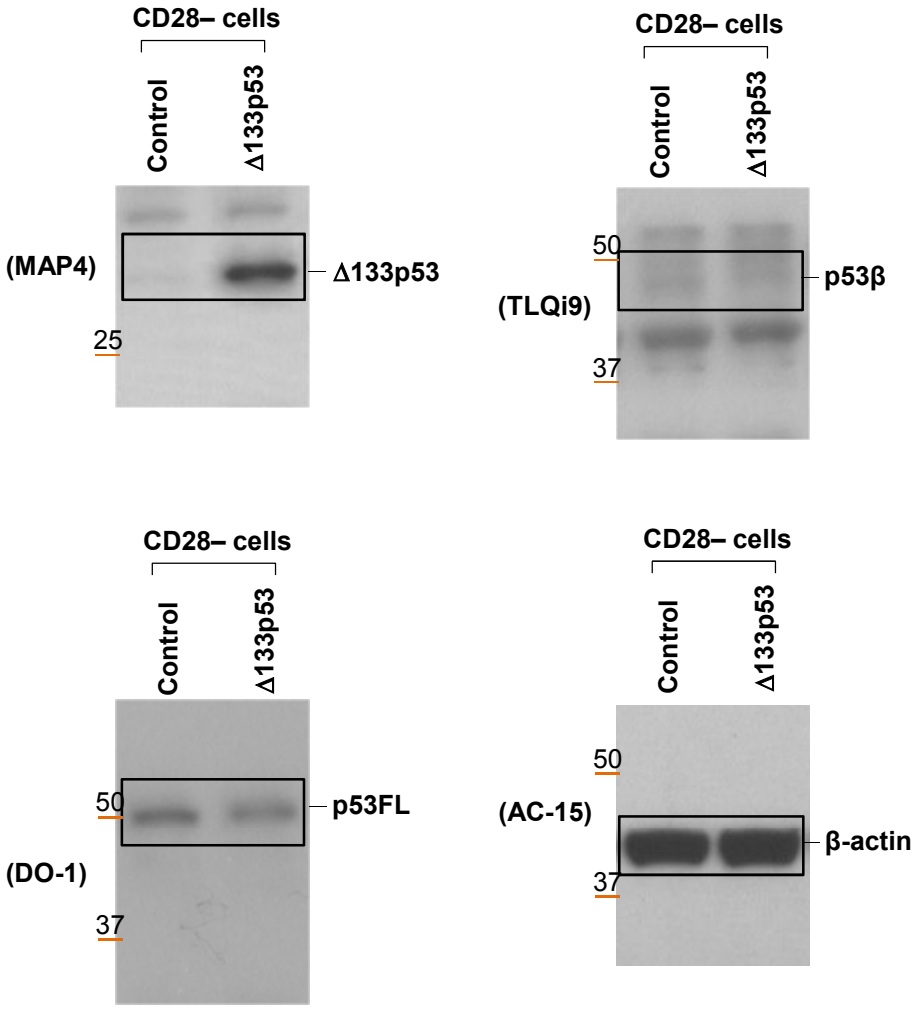

Full scan of immunoblots for Figure 4D

The rectangular areas of the blots were shown in Figure 4D as the results of Δ133p53, p53β and full-length p53 (p53FL) protein levels using MAP4, TLQi9 and DO-1 antibodies, respectively. AC-15 antibody was used to detect β-actin for the loading control.

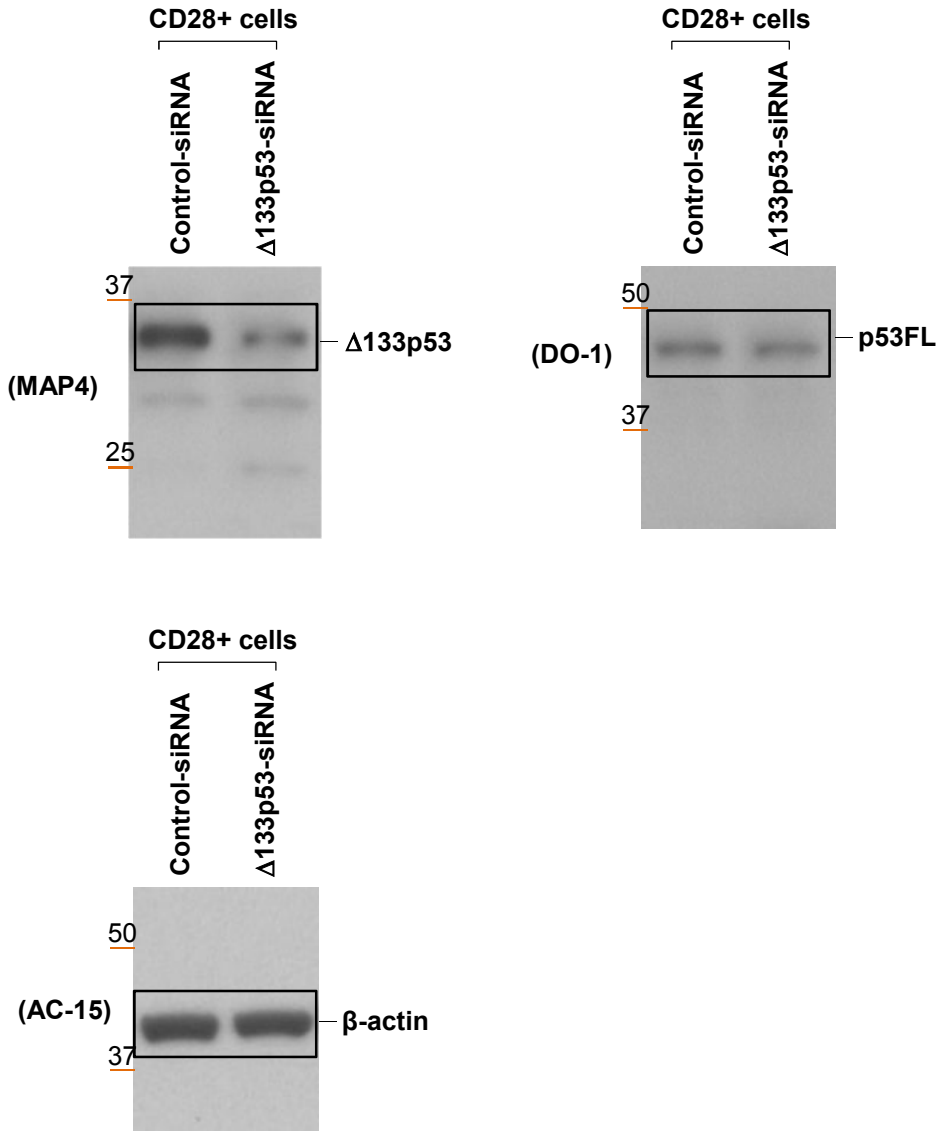

Full scan of immunoblots for Figure 5A

The rectangular areas of the blots were shown in Figure 5A as the results of Δ133p53 and full-length p53 (p53FL) protein levels using MAP4 and DO-1 antibodies, respectively. AC-15 antibody was used to detect β-actin for the loading control.

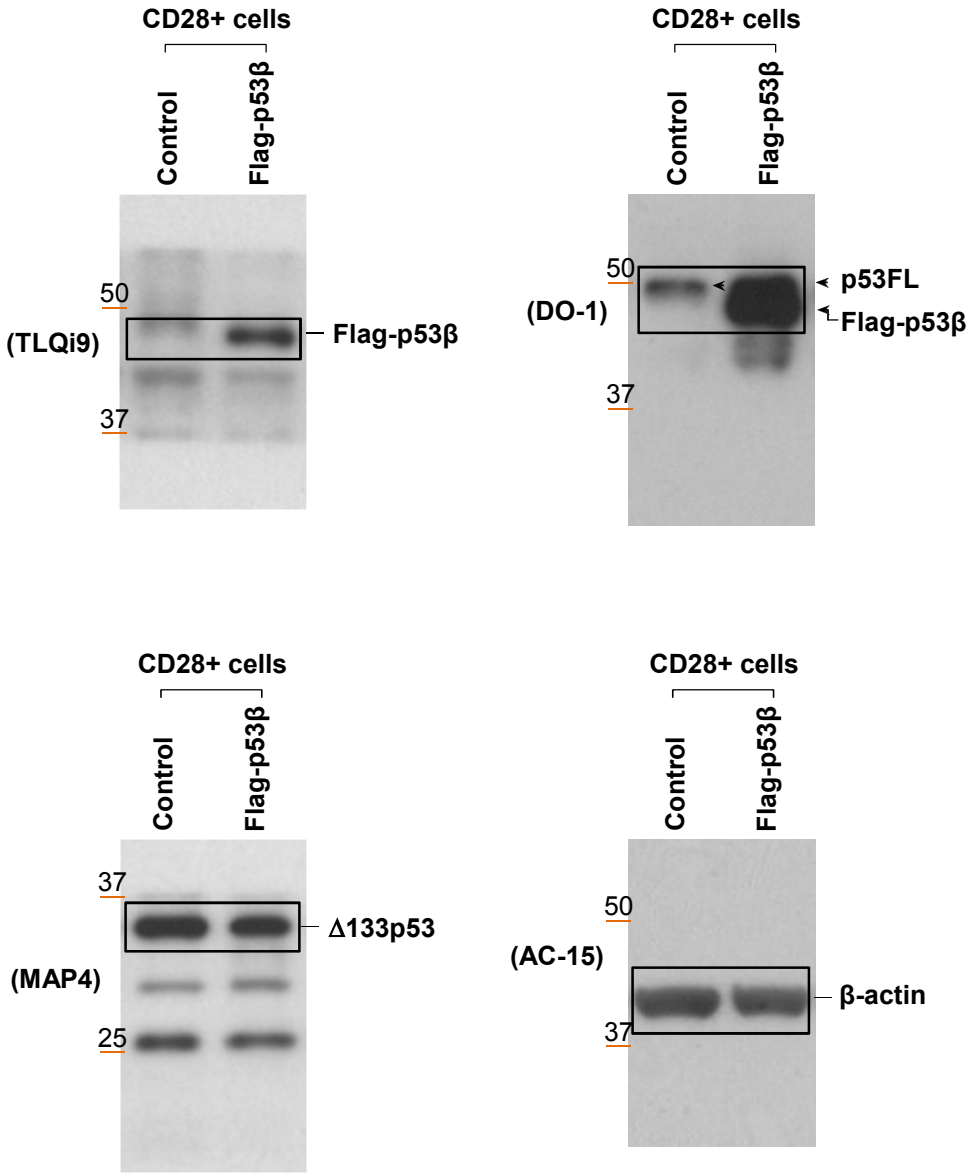

Full scan of immunoblots for Figure 5F

The rectangular areas of the blots were shown in Figure 5F as the results of Flag-p53β, full-length p53 (p53FL) and Δ133p53 and protein levels using TLQi9, DO-1 and MAP4 antibodies, respectively. AC-15 antibody was used to detect β-actin for the loading control.

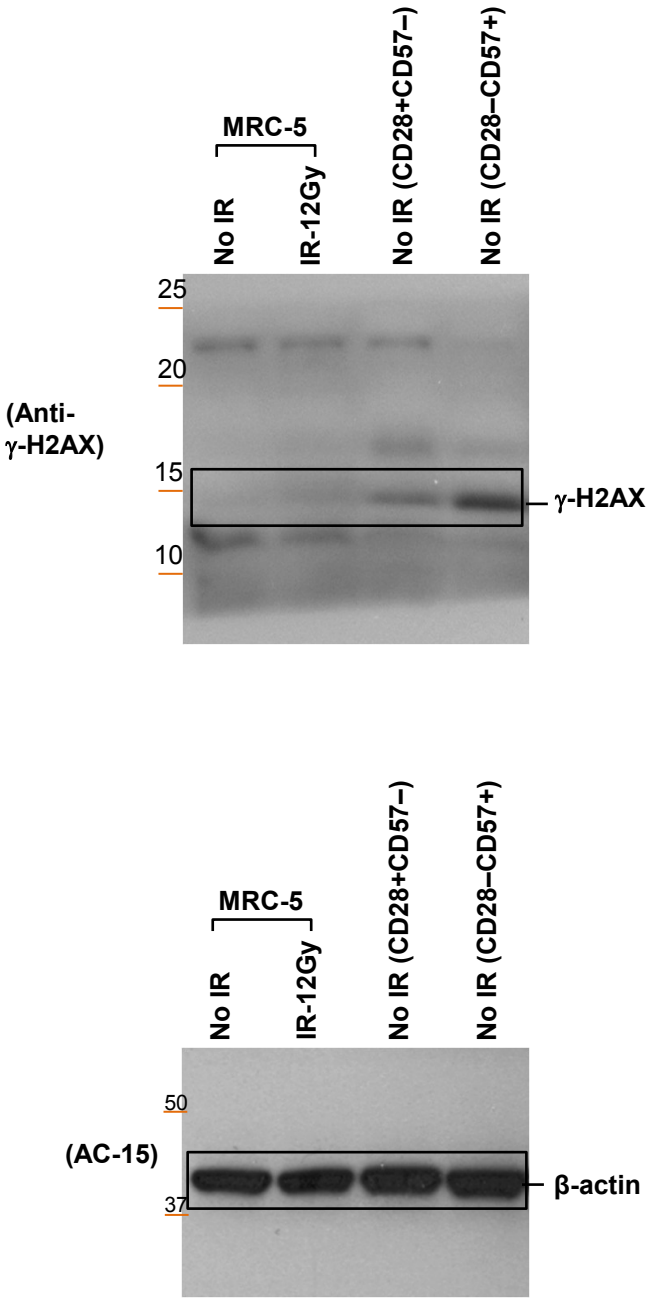

Full scan of immunoblots for Supplemental Figure 4

The rectangular areas of the blots were put together and shown in Supplemental Figure 4 as the results of γ-H2AX protein levels using anti- γ-H2AX antibody. AC-15 antibody was used to detect β-actin for the loading control. The cell lysates loaded were indicated for each lane .

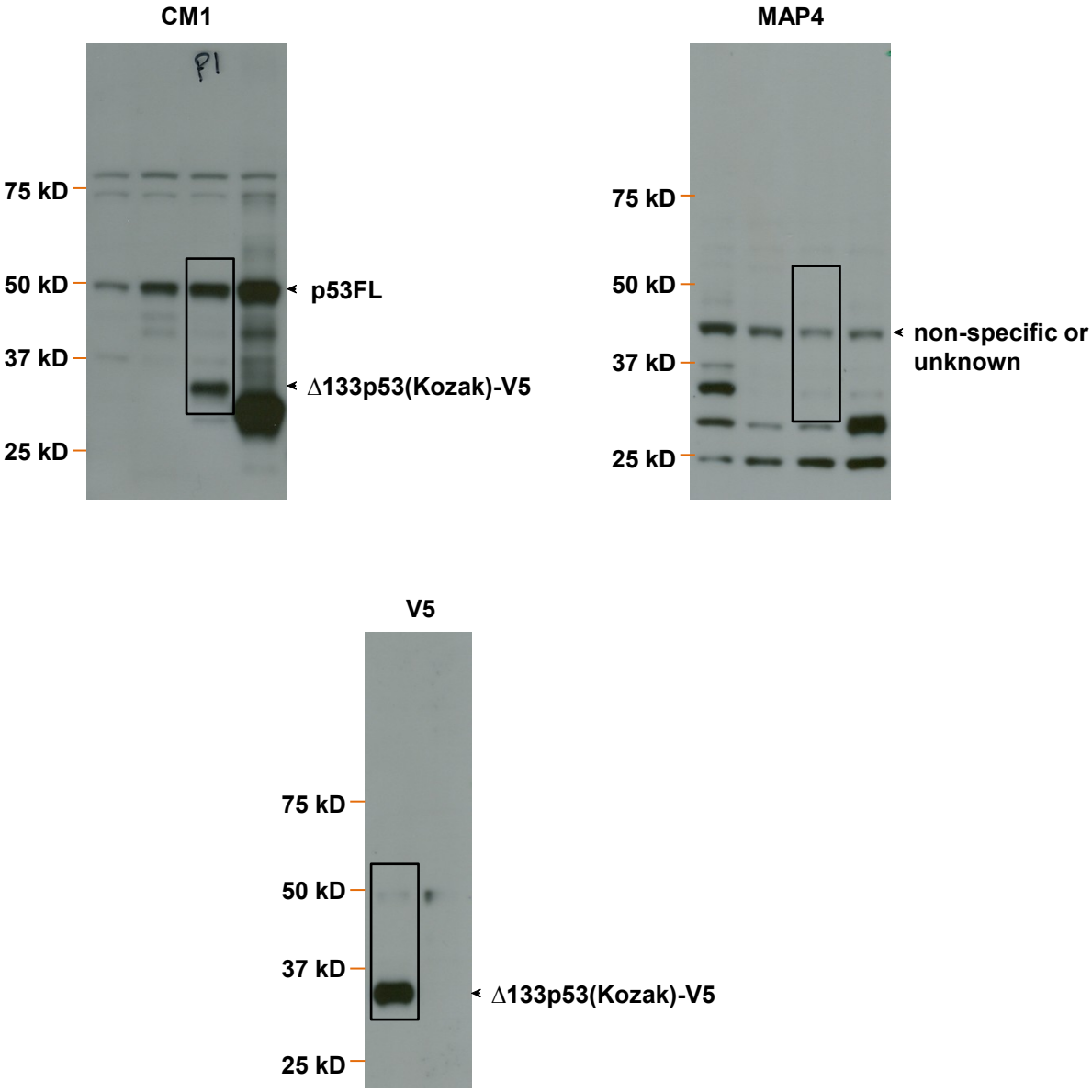

Full scan of immunoblots for Supplemental Figure 6A

The rectangular areas of the blots were put together and shown in Supplemental Figure 6A as the results of full-length p53 (p53FL) and Δ133p53 protein levels using CM1, MAP4 and anti-V5 antibodies.

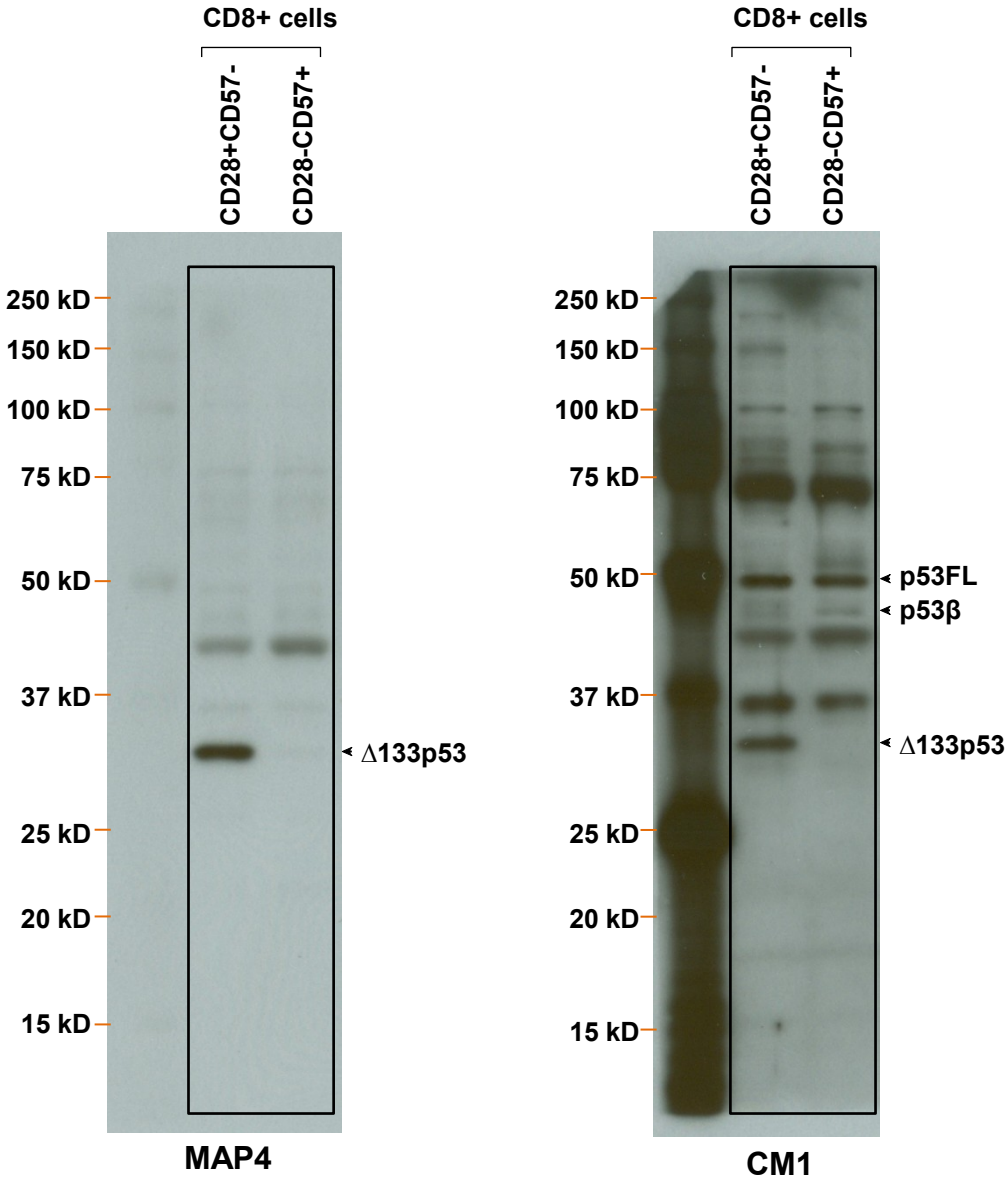

Full scan of immunoblots for Supplemental Figure 6B and C

The rectangular areas of the blots were put together and shown in Supplemental Figure 6B and C as the results of full-length p53 (p53FL) and Δ133p53 protein levels using MAP4 and CM1 antibodies.

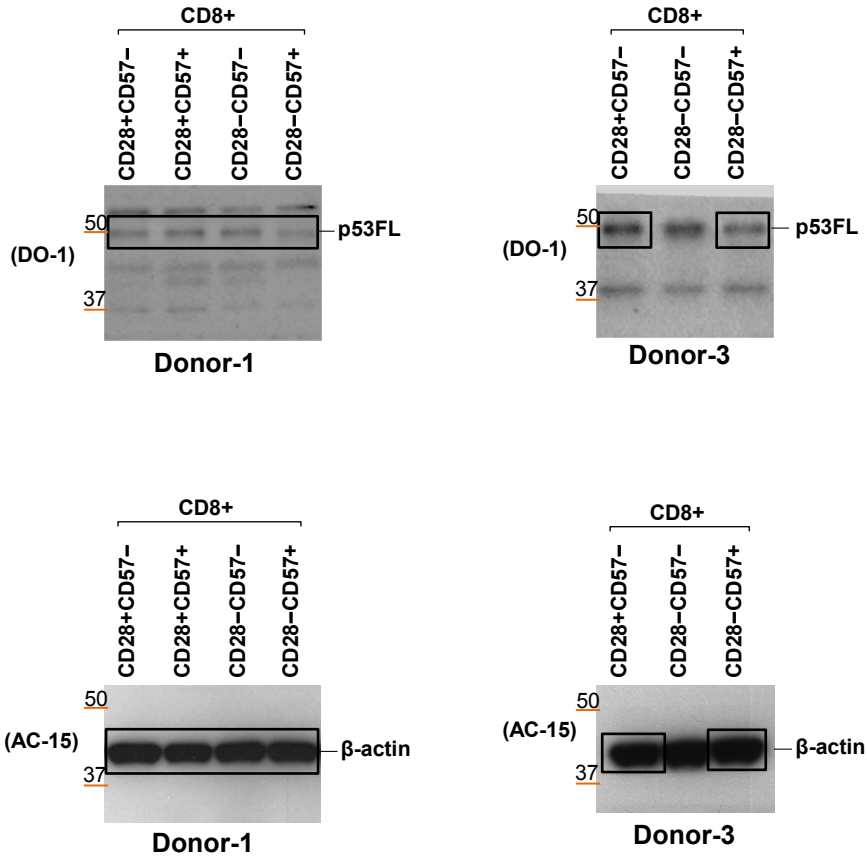

Full scan of immunoblots for Supplementary Figure 7A (Donors 1 and 3)

The rectangular areas of the blots were put together and shown in Supplemental Figure 7A (Donors 1 and 3) as the results of full-length p53 (p53FL) protein levels using DO-1 antibody. AC-15 antibody was used to detect β-actin for the loading control. The cell subsets loaded were indicated for each lane .

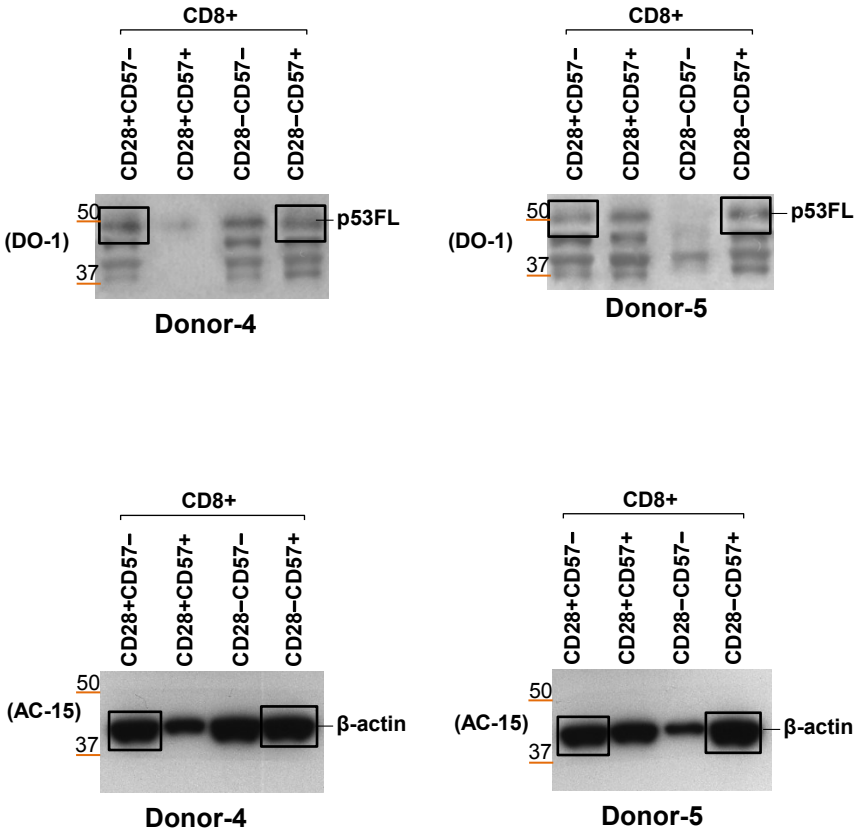

Full scan of immunoblots for Supplementary Figure 7A (Donors 4 and 5)

The rectangular areas of the blots were put together and shown in Supplemental Figure 7A (Donors 4 and 5) as the results of full-length p53 (p53FL) protein levels using DO-1 antibody. AC-15 antibody was used to detect β-actin for the loading control. The cell subsets loaded were indicated for each lane .

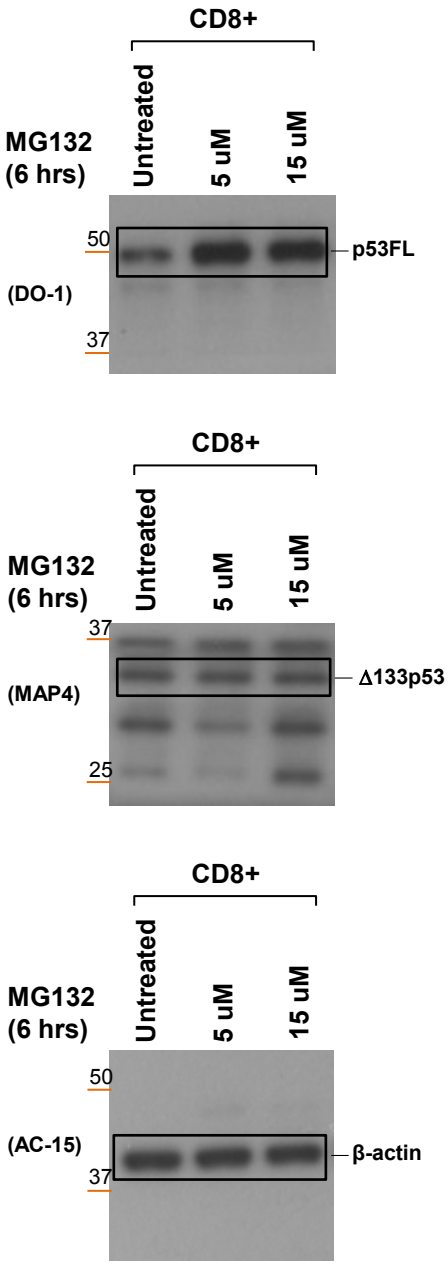

Full scan of immunoblots for Supplementary Figure 8A

The rectangular areas of the blots were put together and shown in Supplemental Figure 8A as the results of full-length p53 (p53FL) and Δ133p53 protein levels using DO-1 and MAP4 antibodies, respectively, after treatment with MG132. AC-15 antibody was used to detect β-actin for the loading control. The cell lysates loaded were indicated for each lane.

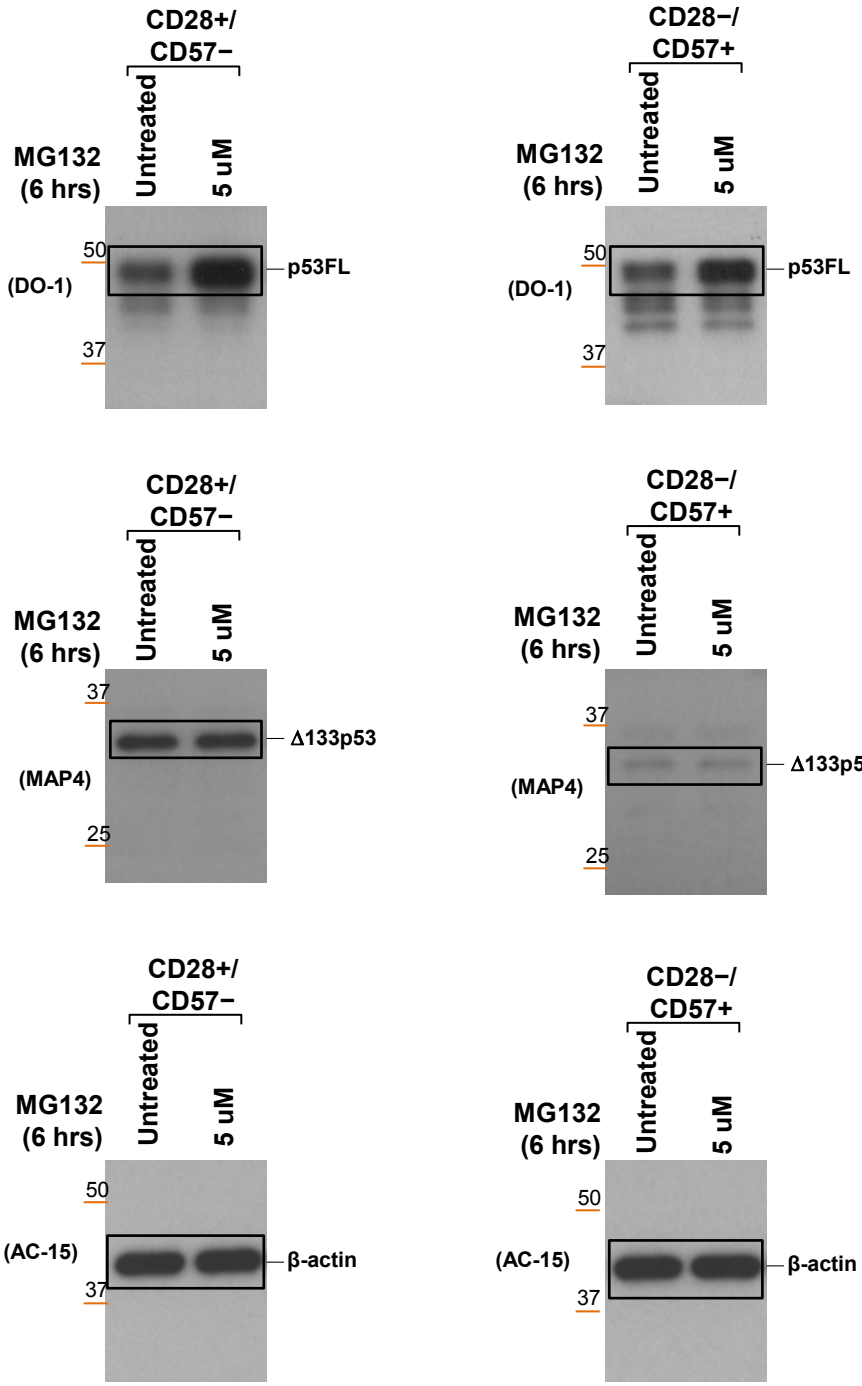

Full scan of immunoblots for Supplementary Figure 8B

The rectangular areas of the blots were put together and shown in Supplemental Figure 8B as the results of full-length p53 (p53FL) and Δ133p53 protein levels using DO-1 and MAP4 antibodies, respectively. AC-15 antibody was used to detect β-actin for the loading control. The cell subsets treated with MG132 and untreated were indicated.

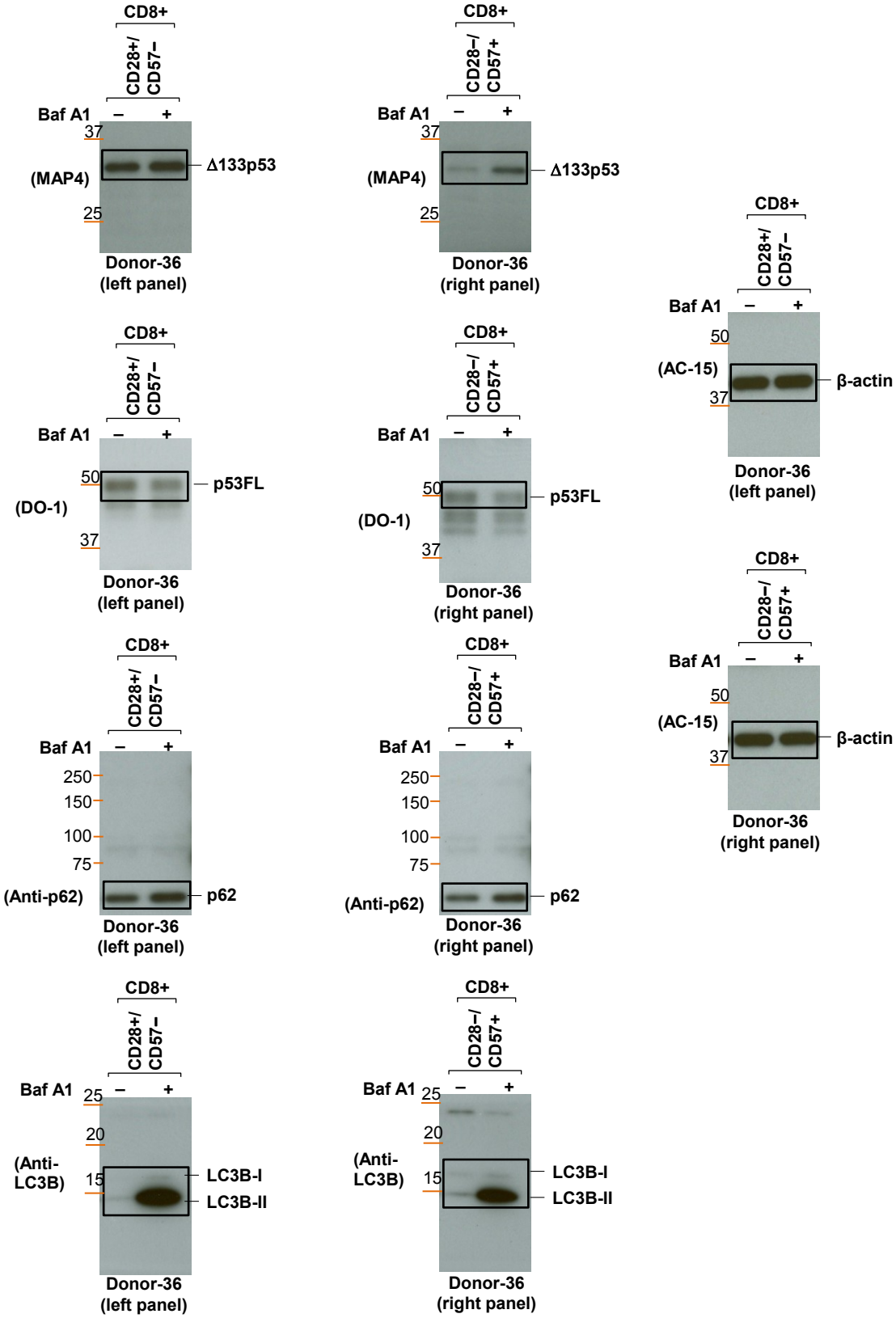

Full scan of immunoblots for Supplementary Figure 8C

The rectangular areas of the blots were put together and shown in Supplemental Figure 8C as the results of full-length p53 (p53FL), Δ133p53, p62 and LC3B protein levels using DO-1, MAP4, anti-p62 and anti-LC3B antibodies, respectively. AC-15 antibody was used to detect β-actin for the loading control. The cell subsets treated with bafilomycin A1 and untreated were indicated.

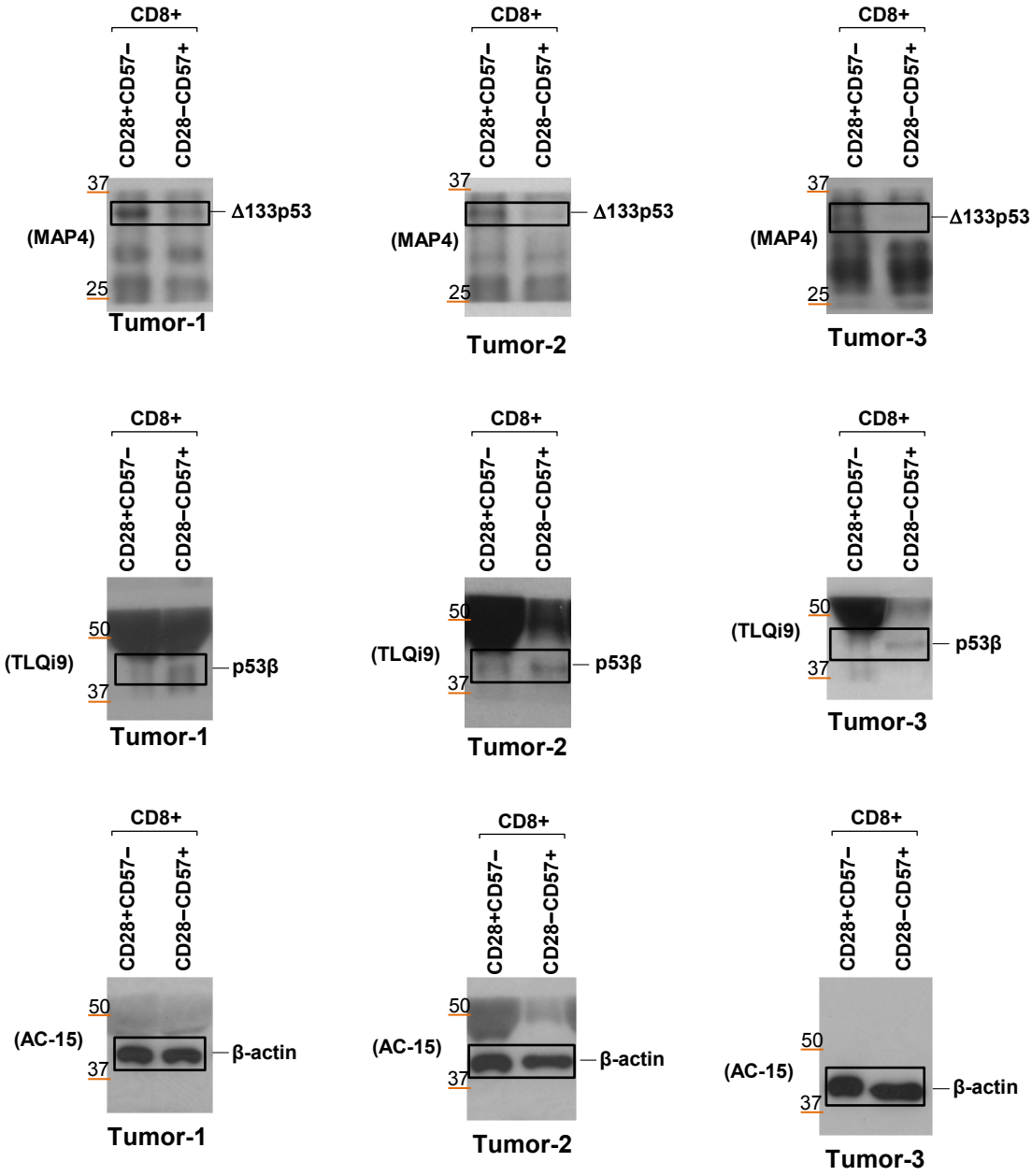

Full scan of immunoblots for Supplementary Figure 9A

The rectangular areas of the blots were put together and shown in Supplemental Figure 9A as the results of Δ133p53 and p53β protein levels using MAP4 and TLQi9 antibodies, respectively. AC-15 antibody was used to detect β-actin for the loading control. The cell subsets loaded were indicated for each lane .

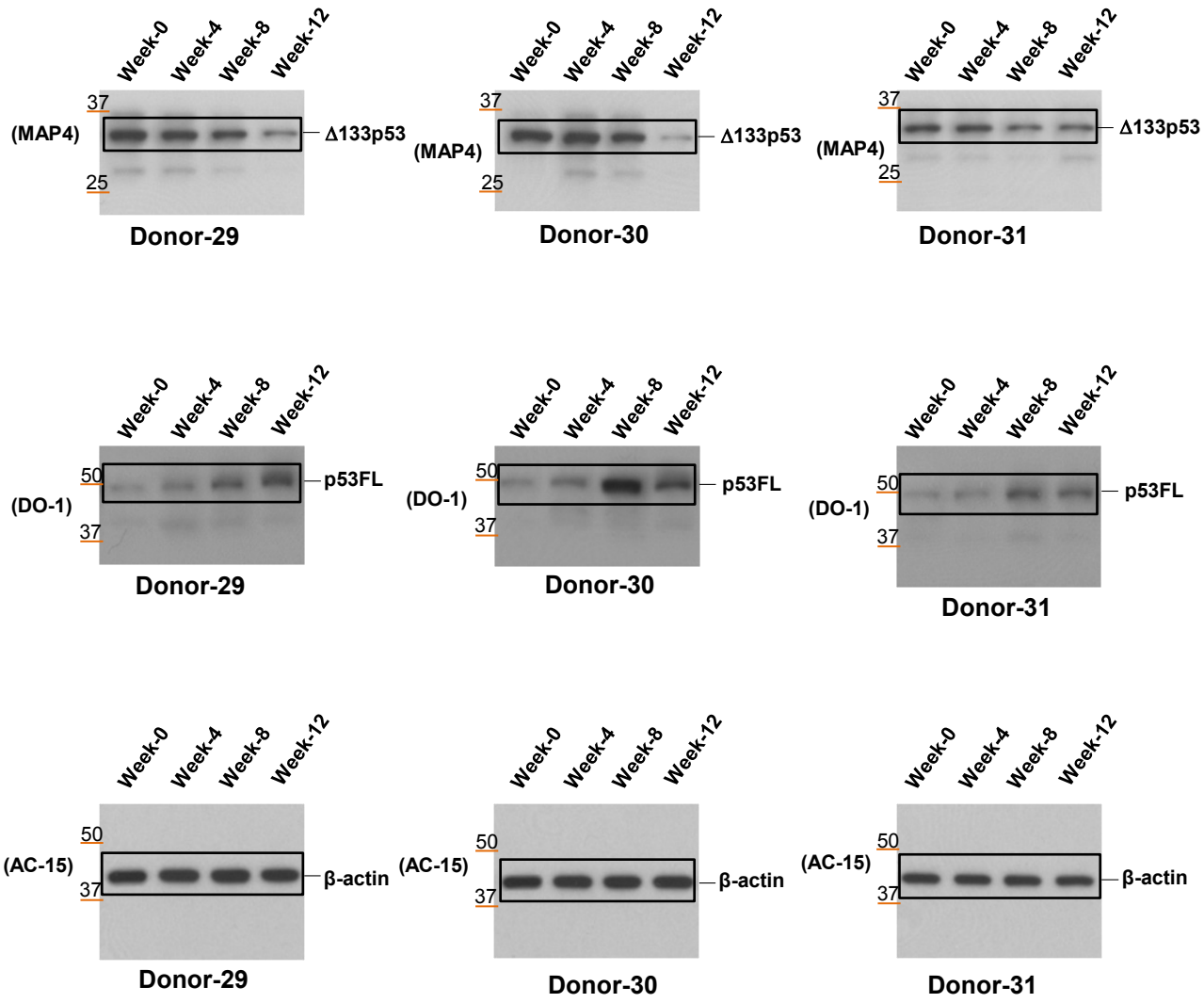

Full scan of immunoblots for Supplementary Figure 10D

The rectangular areas of the blots were put together and shown in Supplemental Figure 10D as the results of Δ133p53 and full-length p53 (p53FL) protein levels using MAP4 and DO-1 antibodies, respectively. AC-15 antibody was used to detect β-actin for the loading control. The cell lysates loaded were indicated for each lane .

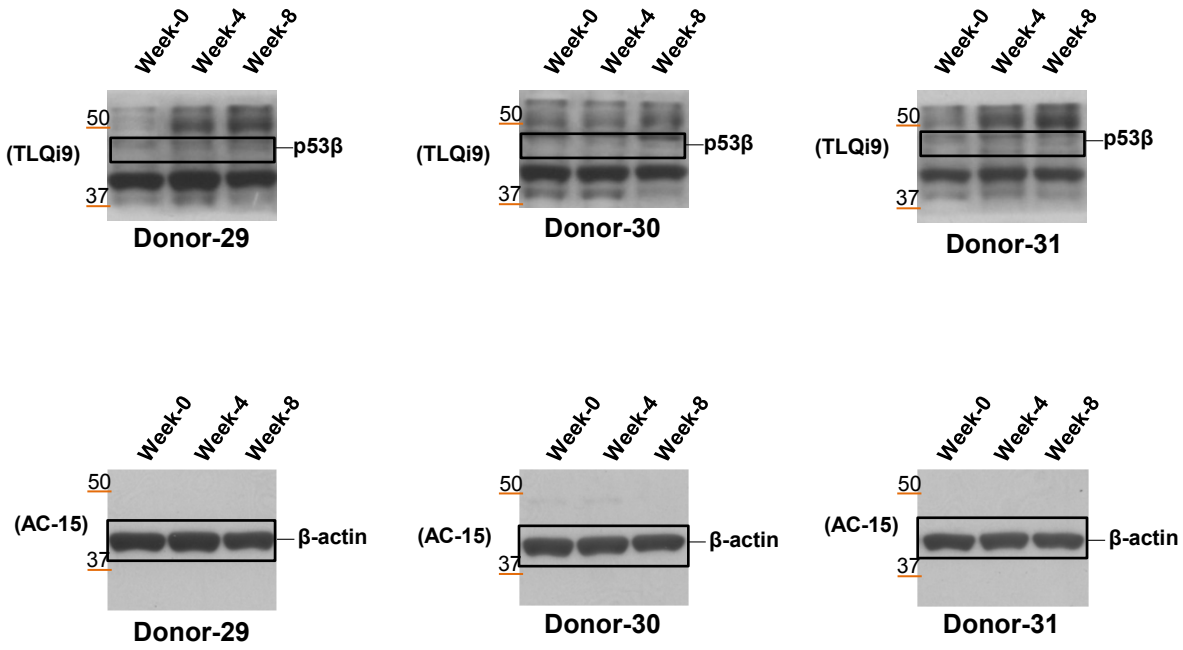

Full scan of immunoblots for Supplementary Figure 10E

The rectangular areas of the blots were put together and shown in Supplemental Figure 10E as the results of p53β protein levels using TLQi9 antibody. AC-15 antibody was used to detect β-actin for the loading control. The cell lysates loaded were indicated for each lane .

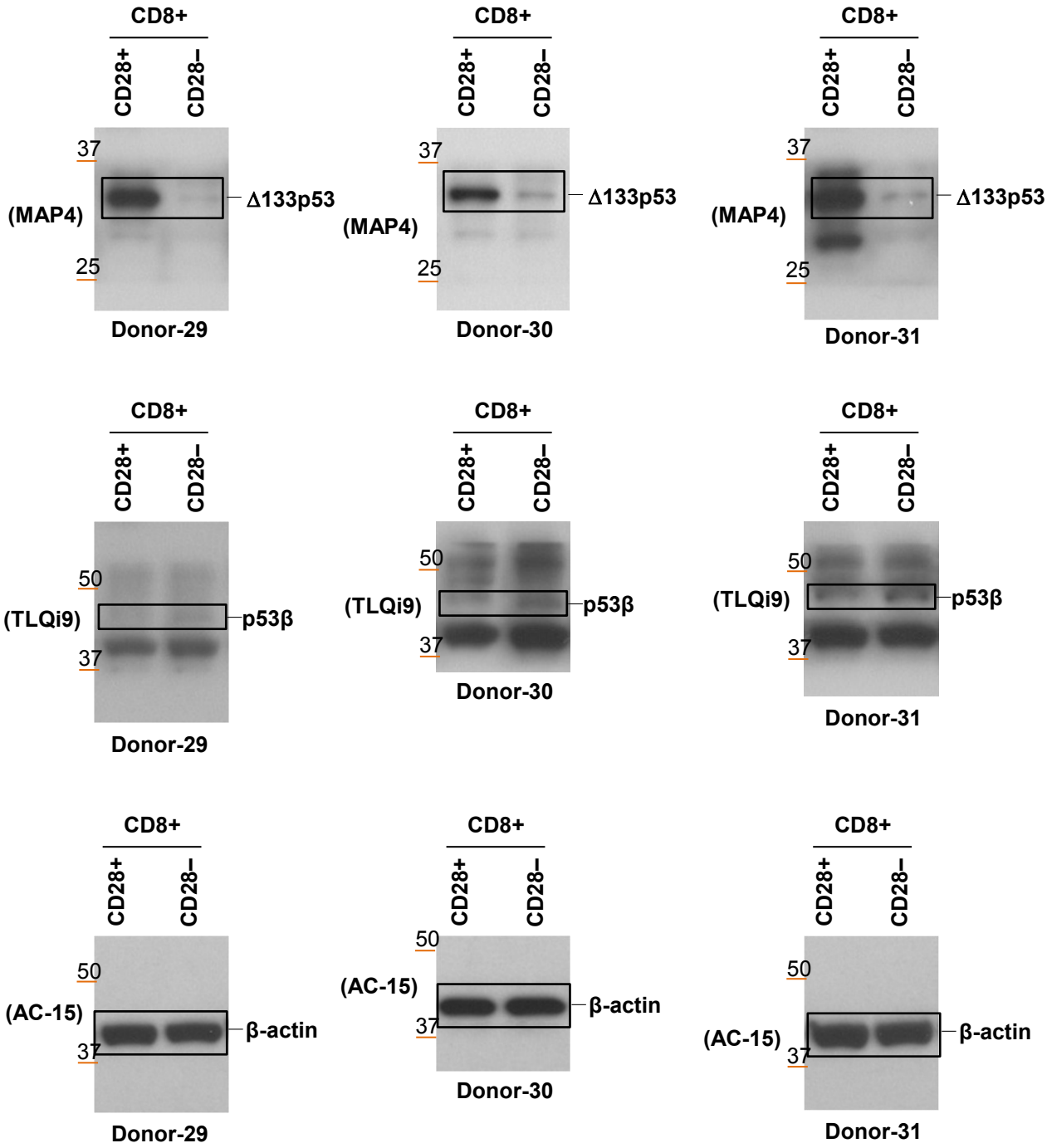

Full scan of immunoblots for Supplementary Figure 11B

The rectangular areas of the blots were put together and shown in Supplemental Figure 11B as the results of Δ133p53 and p53β protein levels using MAP4 and TLQi9 antibodies, respectively. AC-15 antibody was used to detect β-actin for the loading control. The cell subsets loaded were indicated for each lane.

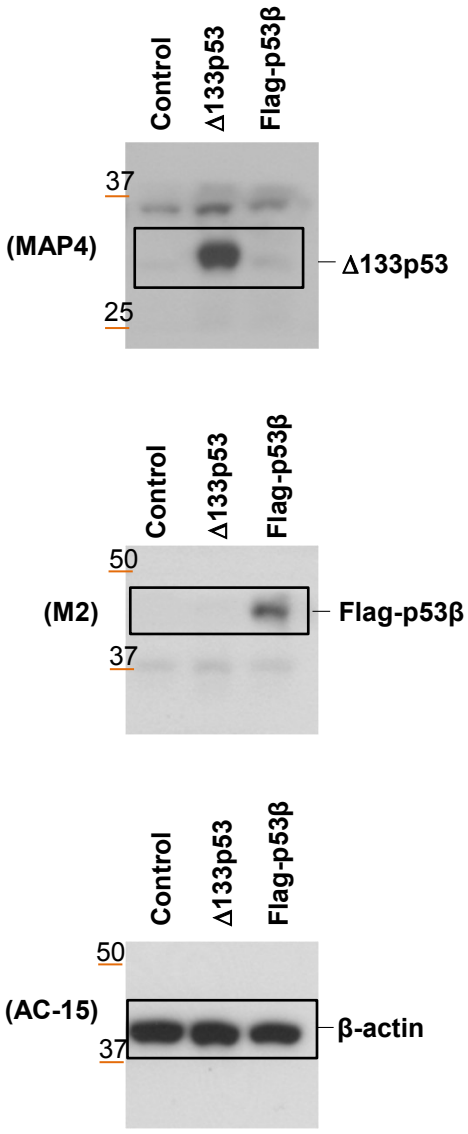

Full scan of immunoblots for Supplementary Figure 13A

The rectangular areas of the blots were put together and shown in Supplemental Figure 13A as the results of Δ133p53 and Flag-tagged p53β protein levels using MAP4 and M2 (anti-Flag) antibodies, respectively. AC-15 antibody was used to detect β-actin for the loading control. The cell lysates loaded were indicated for each lane.

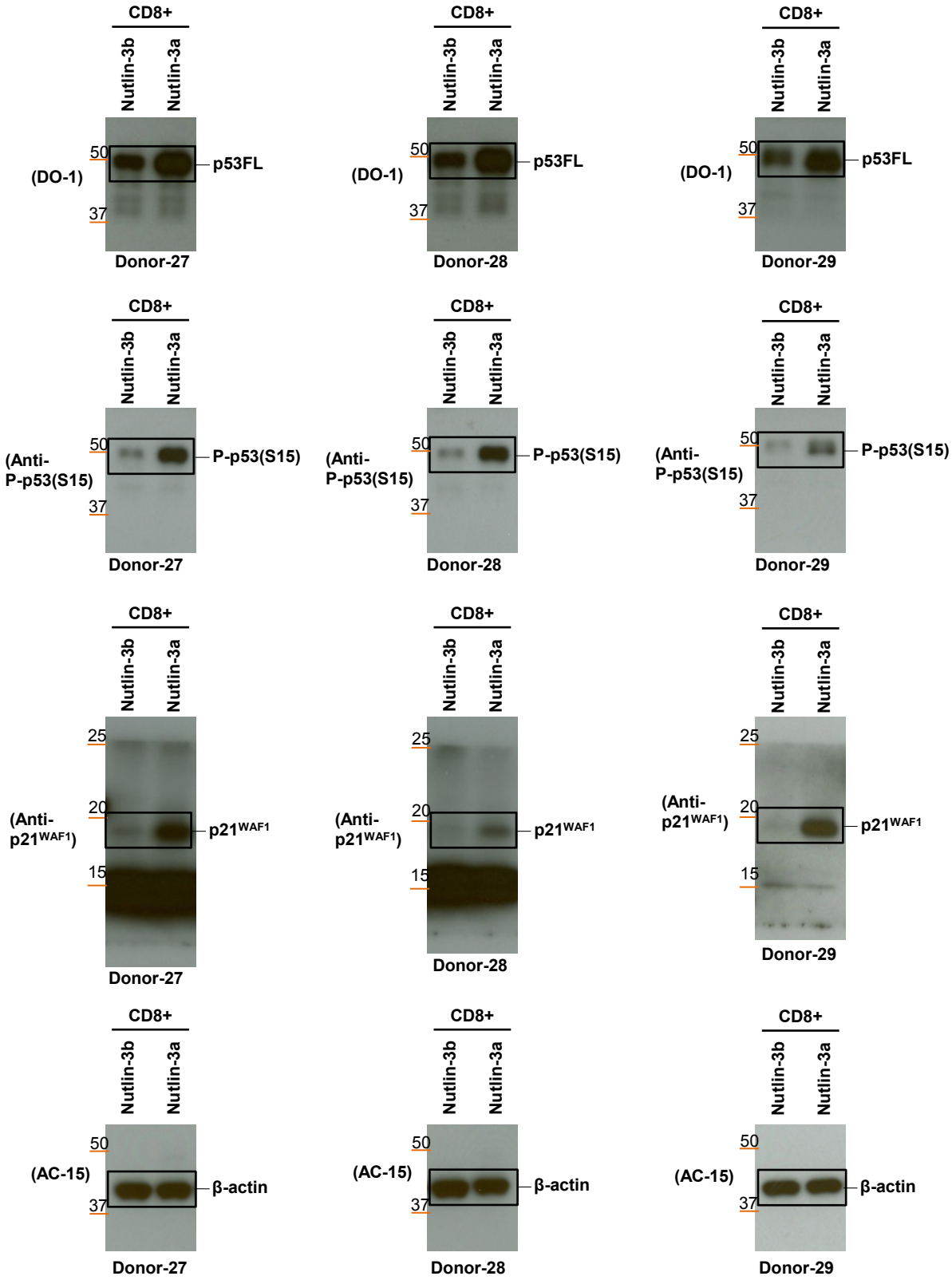

Full scan of immunoblots for Supplementary Figure 15A

The rectangular areas of the blots were put together and shown in Supplemental Figure 15A as the results of full-length p53 (p53FL), phosphorylated p53 [P-p53(s15)], and $p21^{WAF1}$ protein levels using DO-1, anti-P-p53(S15) and anti-$p21^{WAF1}$ antibodies, respectively. AC-15 antibody was used to detect β-actin for the loading control. The cell subsets treated with nutlin-3b and nutlin-3a were indicated.